

AN ABSTRACT OF THE THESIS OF

SOON MO LEE for the MASTER OF SCIENCE
(Name) (Degree)

in MECHANICAL ENGINEERING presented on July 23, 1968
(Major) (Date)

Title: AN EXPERIMENTAL STUDY OF NATURAL CONVECTION IN
AIR BETWEEN A VERTICAL ISOTHERMAL HOT PLATE AND A
PARALLEL INSULATED PLATE

Abstract approved: _____

Dr. James R. Welty

The free convective heat transfer phenomena in air between two vertical plates 24 by 38 inches spaced 15.895 mm apart, was investigated in this experimental study. One plate was isothermal and the other adiabatic.

A quartz fiber anemometer was used for measuring local velocities in the air between the vertical plates. A very fine iron-constantan thermocouple was used for local temperature measurements. Velocity and temperature profiles were obtained at several vertical positions along the plates.

With the data obtained, local and mean convective heat transfer coefficients were determined at each vertical position.

An Experimental Study of Natural Convection in Air
Between a Vertical Isothermal Flat Plate
And a Parallel Insulated Flat Plate

by

Soon Mo Lee

A THESIS

submitted to

Oregon State University

in partial fulfillment of
the requirements for the
degree of

Master of Science

June 1969

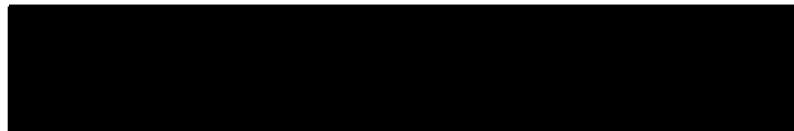
APPROVED:



Professor of Mechanical Engineering
in charge of major



Head of Department of Mechanical Engineering



Dean of Graduate School

Date thesis is presented July 23, 1968

Typed by Marion F. Palmateer for Soon Mo Lee

ACKNOWLEDGMENT

The author wishes to thank Dr. J. R. Welty for his personal guidance throughout my graduate study program and for his valuable suggestions in writing this thesis.

To the personnel of the Department of Mechanical Engineering of Oregon State University who assisted the author, but are too numerous to mention individually, the author also expresses his sincere thanks.

A special form of gratitude is reserved for the financial support, during the two past years, of my parents who are in Korea. I wish, also, to express my thanks for the understanding of my wife who has just arrived in this country. Her patience and understanding during my course of study has been a great inspiration to my work.

My gratitude is extended to my fellow graduate students who have become my good friends. Through them I feel that I have received a second education with respect to the culture and social aspects of the United States and her people.

TABLE OF CONTENTS

	<u>Page</u>
INTRODUCTION	1
THEORETICAL BACKGROUND	3
Vertical Rectangular Cells	4
DISCUSSION OF APPARATUS AND TEST	24
General	24
Positioning of the Vertical Plates	25
Hot Plate Assembly	28
Adiabatic Plate Assembly	29
Heat Reservoir	29
Power Level	31
Pressure Measurement	31
Millivolt Potentiometer	31
Aspirator	31
Calibration of the Velocity Measuring Instrument	33
RESULTS AND CONCLUSIONS	39
Velocity Measurements	39
Temperature Measurements	44
CONCLUSIONS	58
BIBLIOGRAPHY	59
APPENDIX	61

LIST OF FIGURES

<u>Figure</u>		<u>Page</u>
1	Overall dimensions of the vertical plates.	5
2	Various flow regimes for rectangular enclosure.	7
3	Solution of differential equations (23) and (24) for $Pr = .733$ (from Schmidt and Beckmann (9)).	19
4	Scheme of two vertical plates.	26
5	Whole view of apparatus.	27
6	Positions of thermocouples on hot plate.	28
7	Local temperatures on the hot surface.	30
8	Millivolt potentiometer top view.	32
9	Scheme of calibration apparatus of quartz fiber.	34
10	Wet test precision meter and air pump.	36
11	Scheme of quartz fiber.	37
12	Graph of quartz fiber calibration.	38
13	Dimensionless velocity profiles.	40
14	Temperature profiles.	45
15	Dimensionless temperature profiles.	46
16	Graphical determination of $\frac{d\theta}{d(\frac{y}{L})}_{y=0}$	51
17	Local Nusselt number as a function of vertical position.	53
18	Local Nusselt number variation with $(N_{Gr})_L \times x/H$.	54
19	Local average temperature vs. vertical position.	56

LIST OF TABLES

<u>Table</u>		<u>Page</u>
1	Calibration data for quartz fiber.	61
2	Experimental velocity data.	65
3	Temperature data.	75
4	Local Nusselt numbers at various vertical positions.	85
5	Local Grashof numbers at various vertical positions.	85

NOMENCLATURE

A	heat transfer area
c_p	specific heat
g	gravitational acceleration
h	convective heat transfer coefficient
H	total height of vertical plate
k	conductivity of fluid
L	distance between plates
N	number
P	pressure
q	heat transferred
t	time
T	temperature
U	velocity component in x-direction
V	velocity component in y-direction
W	width of plate
x	direction tangent to the heated plate
y	direction normal to the heated plate

Parameters

Gr_L Grashof number $\frac{\beta g L^3}{\nu^2} (T_s - T_\infty)$

Nu_L Nusselt number $\frac{hL}{K}$

Pr prndtl number $C_p \mu / K$.

Greek Symbols

α	thermal diffusivity
β	coefficient of volumetric expansion
δ	increment
θ	dimensionless temperature
μ	absolute (or dynamic) viscosity
ψ	stream function
ρ	density
η	dimensionless length
ϕ	dissipation function
ν	kinematic viscosity

Subscripts

a	adiabatic wall
c	cold surface
f	fluid (between plates)
h	hot
L	air layer thickness
s	surface (hot surface)
∞	reference conditions for plate

Superscripts

$'$	first derivative
$''$	second derivative
$'''$	third derivatives

AN EXPERIMENTAL STUDY OF NATURAL CONVECTION IN AIR BETWEEN A VERTICAL ISOTHERMAL FLAT PLATE AND A PARALLEL INSULATED FLAT PLATE

INTRODUCTION

This thesis deals with natural convection between two vertical plates one being an isothermal hot plate and the other an adiabatic plate.

Heat is transmitted across a confined air space by convection, conduction and radiation. It has been customary to regard each of these modes as independent but, in this investigation, it was found impractical to separate conduction and convection. These two modes may be conveniently designated by the term diffusion. Part of the heat is transferred by diffusion; the remainder is transferred by radiation in accordance with the familiar Stefan-Boltzman law.

It has been demonstrated by means of numerous experiments that heat transfer by natural or free convection varies approximately with the $5/4$ power of the temperature difference between a surface and its adjacent fluid. For the temperature differences usually found in building walls, the transfer of heat by both conduction and radiation is approximately proportional to the temperature difference.

In a theoretical study of convection, the partial differential equations governing fluid motion are complicated, and it is natural that their analytical solution becomes difficult or even impossible

unless considerable simplifications are made.

The first experimental heat transfer studies related to vertical plates were initiated in the late nineteenth century. Since then experimental studies have been expanded to include the use of various fluids under the influence of both constant heat flux and isothermal conditions.

The purpose of this work is to investigate the temperature and velocity variations in air at various locations within the laminar flow range between a vertical isothermal plane and an insulated parallel plate, and to evaluate local heat transfer coefficients along the heated wall.

■

THEORETICAL BACKGROUND

Convective heat transfer is the transport of energy to or from a surface by both molecular conduction processes and gross fluid movement. If the fluid motion involved in the process is induced by some external means (pump, blower, wind, vehicle motion, etc.), the process is called forced convection. If the fluid motion arises from external force fields, such as gravity associated with the density gradients induced by the transport itself, we usually call the process free convection.

In the case of free convection, there is superimposed on the fluid flow field a flow of heat, thus the flow field interacts with the temperature field. In order to determine the temperature distribution it is necessary to combine the equations of motion with those of heat transfer. It is intuitively evident that the temperature distribution around a hot body which is placed in a fluid stream and which is heated so that its temperature is maintained above that of the surroundings will be such that the temperature of the stream will increase close to the body.

Throughout this discussion, reference will be made to distances along and normal to the heated plane wall. In order to avoid confusion in this matter, the point $y = 0$, $x = 0$ refers to the bottom of the heated plate, the positive x -axis is parallel to the

heated plate, and the positive y-axis is defined to be normal to the heated plate.

Vertical Rectangular Cells

Consider the vertical layer shown in Figure 1 with dimensions L, W and H. By means of dimensional analysis, it can be shown that the heat transferred across such layers is a function of the Grashof number, the Prandtl number, the fluid layer-to-height ratio and the width-to-height ratio. The dimensionless heat transfer coefficient, the Nusselt number, can be written as a function of these quantities:

$$Nu = f(Gr, Pr, H/L, W/L)$$

where

$Nu = hL/k$, the Nusselt number,

$$Gr = \frac{\beta g L^3 (T_H - T_C)}{\nu^2}, \text{ Grashof number,}$$

H = height of vertical plane wall,

L = air layer

W = width of vertical plane wall,

$Pr = \mu C_p / k$, Prandtl number

For fluid layers that are sufficiently large in the z direction, the Nusselt number is independent of the W/L ratio and the layer can be considered as plane.

- A Hot wall
- B Box with vapor acetone
- C Adiabatic wall
- D Vapor acetone
- E Liquid acetone

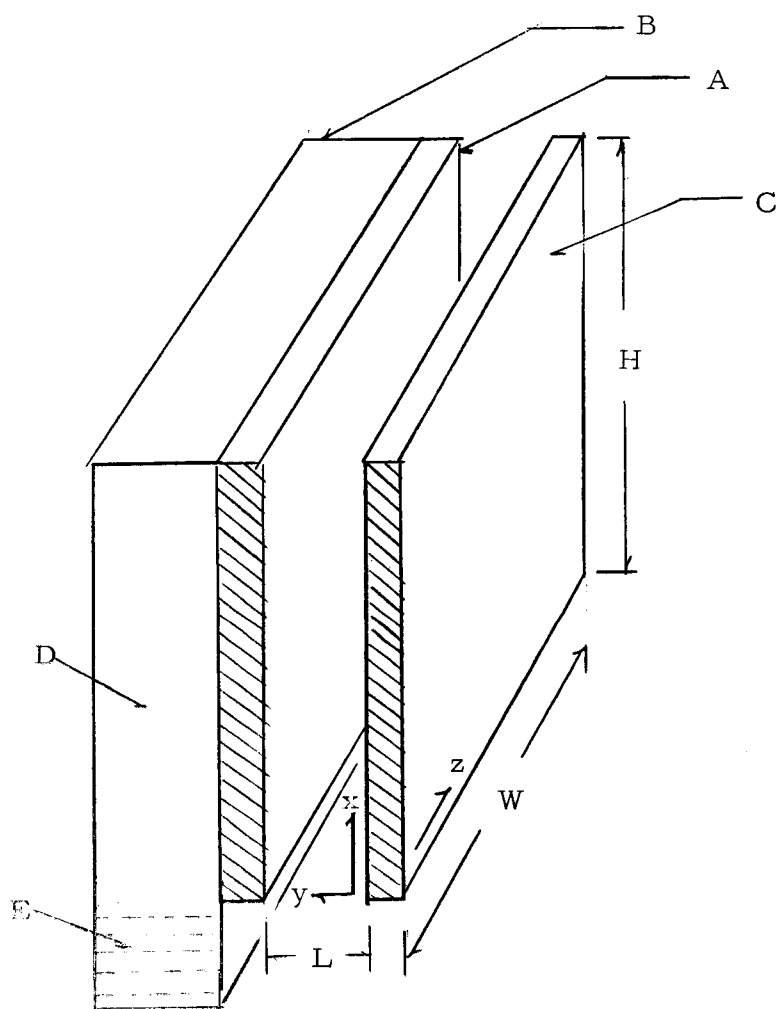


Figure 1. Overall dimensions of the vertical plates.

In order to complete the description of flow, characteristic temperature and velocity profiles are shown in Figure 2 for those regions considered in this thesis. A written description of the mechanisms which create the various flow regimes follows.

Consider air in the space between the isothermal hot plate and the adiabatic plate. The heated plate is at temperature, T_h , and the other is at a lower temperature, T_c (T_c is not constant).

For small temperature differences, buoyancy effects are small or non-existent and, therefore, heat transfer is primarily by conduction. Temperature profiles are linear throughout most of the region except possibly for that portion of the fluid subjected to end effects; velocities are small.

As the temperature difference increases, the convective effects become more pronounced. With Grashof numbers on the order of 10^7 , convective effects completely dominate. At a point beyond about 20 in. from the bottom edge of the heated plate, a transition to turbulent flow occurs with completely turbulent flow occurring above a Grashof number of approximately 10^{10} .

For the situations involving Grashof numbers above the transition value, boundary layer integral techniques have been applied, resulting in adequate correlations with experimental data.

In all cases radiation may be present, but its contribution is negligible at moderate temperatures, and we shall neglect it

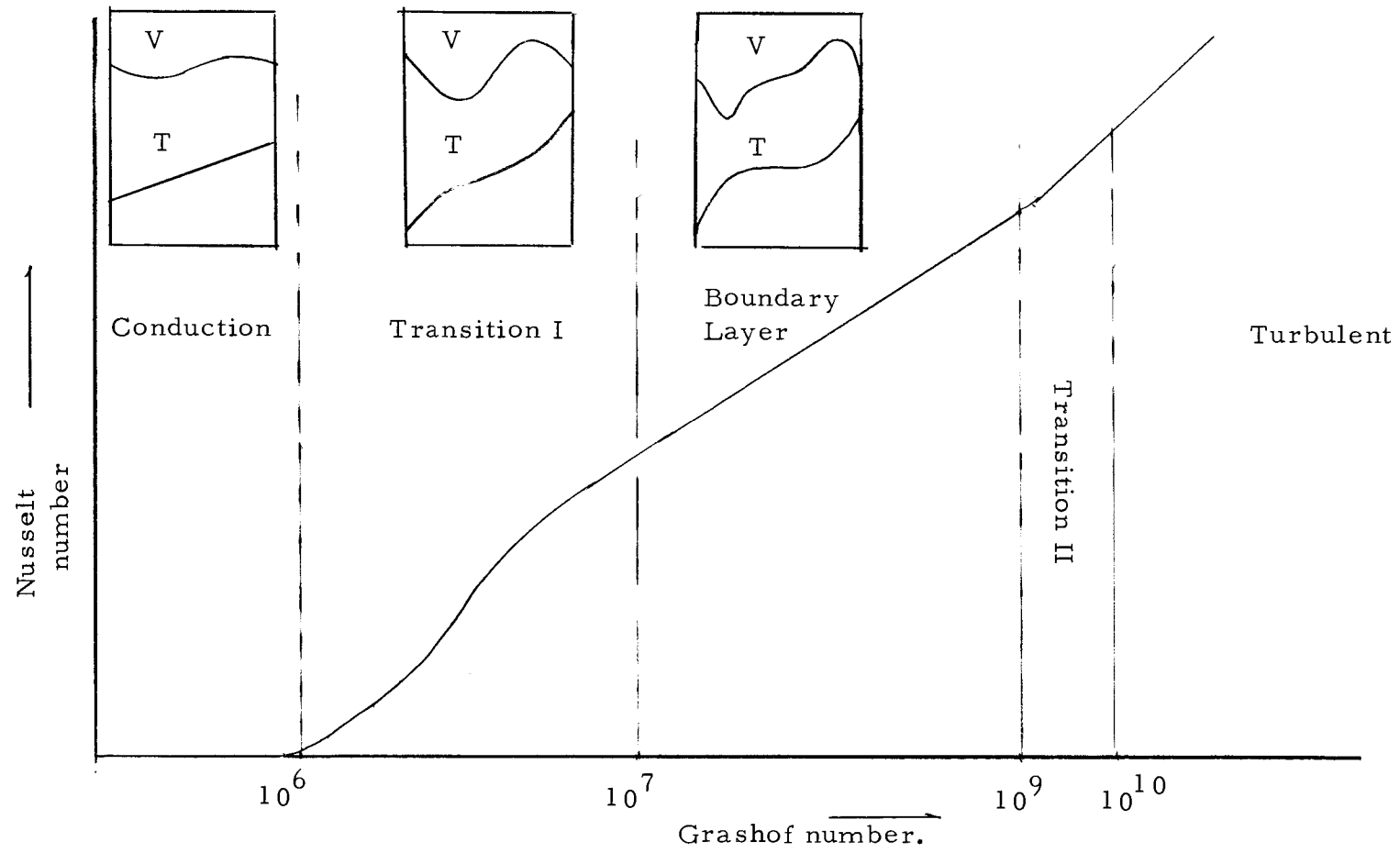


Figure 2. Various flow regimes for rectangular enclosure.

completely.

The energy equation, in differential form, which applies is

$$\rho c_p \frac{DT}{Dt} = \frac{DP}{Dt} + K \nabla^2 T + \mu \phi$$

where ϕ denotes the dissipation function, which, in the case of laminar flow is

$$\begin{aligned} \phi = & 2 \left[\left(\frac{\partial U}{\partial x} \right)^2 + \left(\frac{\partial V}{\partial y} \right)^2 + \left(\frac{\partial W}{\partial z} \right)^2 \right] + \left(\frac{\partial V}{\partial x} + \frac{\partial U}{\partial y} \right)^2 + \left(\frac{\partial W}{\partial y} + \frac{\partial V}{\partial z} \right)^2 \\ & + \left(\frac{\partial U}{\partial z} + \frac{\partial W}{\partial x} \right)^2 - \frac{2}{3} \left(\frac{\partial U}{\partial x} + \frac{\partial V}{\partial y} + \frac{\partial W}{\partial z} \right)^2 \end{aligned}$$

For the situation studied the pressure was held constant, thus

$DP/Dt = 0$, and the energy equation reduces to

$$\rho c_p \frac{DT}{Dt} = K \nabla^2 T + \mu \phi$$

Motions which are caused solely by the density gradients created by temperature difference are termed, "natural convection" as distinct from these "forced" on the stream by external causes. Such a natural flow exists around a vertical hot plate or around a horizontal hot cylinder. Natural flow also displays, in most cases, a boundary layer structure particularly if the viscosity and conductivity are small.

In the case of the vertical hot plate, the pressure in each horizontal plane is equal to the hydrostatic pressure, and is thus constant

for a fluid of low density such as air.

Fluid motion results from the difference between weight and buoyancy forces due to density differences resulting from heat transfer.

The heat transfer between a vertical wall and air surrounding it was the first natural convection problem to be solved analytically. This was achieved by L. Lorenz in 1881 (4). In order to simplify the problem, he made the following assumptions:

1. The free convection took place under steady-state conditions.
2. The temperature T at the surface of the vertical wall was uniform and constant.
3. The temperature T of the surrounding air at a distance from the vertical surface was uniform and constant.
4. The horizontal component V of the air velocity was neglected.
5. Both the temperature T and the velocity component U measured from the surface of the wall, and of the vertical distance x measured from the bottom of the wall.
6. The force of the gravity was the only force acting on the air.
7. The pressure at any given horizontal plane was uniform and constant.
8. The variation of pressure in the vertical direction was so

small that the mass density of air dependent on temperature only.

9. The specific heat c_p , dynamic viscosity, and the thermal conductivity K of air were considered as constant within the range of temperature involved.

Then under the steady state conditions, the equation of motion of air is

$$\rho U \frac{\partial U}{\partial x} = \mu \left(\frac{\partial^2 U}{\partial x^2} + \frac{\partial^2 U}{\partial y^2} \right) + (\rho_\infty - \rho)g \quad (1)$$

and the equation of heat flow is

$$\rho c_p U \frac{\partial T}{\partial x} = K \left(\frac{\partial^2 T}{\partial x^2} + \frac{\partial^2 T}{\partial y^2} \right) \quad (2)$$

Since $\rho/\rho_\infty = T_\infty/T$ where T_∞ and T are absolute temperature, since $\rho = \rho_\infty (T_\infty/T)$ the equation (1) becomes

$$\frac{T_\infty}{T} \rho_\infty U \frac{\partial U}{\partial x} = \mu \left(\frac{\partial^2 U}{\partial x^2} + \frac{\partial^2 U}{\partial y^2} \right) + \rho_\infty \frac{T - T_\infty}{T} g$$

or

$$U \frac{\partial U}{\partial x} = \frac{\mu}{\rho_\infty} \frac{T}{T_\infty} \left(\frac{\partial^2 U}{\partial x^2} + \frac{\partial^2 U}{\partial y^2} \right) + \frac{T - T_\infty}{T_\infty} g \quad (3)$$

and equation (2) becomes

$$U \frac{\partial T}{\partial x} = \frac{K}{\rho_\infty c_p} \frac{T}{T_\infty} \left(\frac{\partial^2 T}{\partial x^2} + \frac{\partial^2 T}{\partial y^2} \right) \quad (4)$$

To reduce these two equations further, Lorenz made the following additional assumptions:

1'. The vertical velocity U remained constant in any vertical plane parallel to the wall so that $\frac{\partial U}{\partial x} = 0$

2'. The coefficients $(\mu/\rho_\infty)(T/T_\infty)$ and $(K/\rho_\infty c_p)(T/T_\infty)$ were considered constant, and difference between T and T_∞ was so small in comparison with the absolute temperature T that the ratio, T/T_∞ , in the coefficients was considered equal to unity.

3'. At the upper edge of the vertical wall where $x = H$ feet, the vertical velocity, U , and the temperature were both considered as constant.

4'. Both sides of equation (4) were multiplied by dx/H so that the term at the left side of equation (4) was integrated to yield UT/H .

5'. The change of T with respect to the vertical distance was so small that T was almost constant in any vertical plane parallel to the wall, and the term $\partial^2 T / \partial x^2$ on the right side of equation (4) was neglected.

Consequently equations (3) and (4) become respectively

$$0 = \frac{\mu}{\rho_\infty} \frac{\partial^2 U}{\partial y^2} + \frac{T - T_\infty}{T} g \quad (5)$$

and

$$\frac{UT}{H} = \frac{K}{\rho_\infty c_p} \frac{d^2 T}{dy^2} \quad (6)$$

The boundary conditions are

$$\text{at } y = 0 \quad T = T_2 \text{ and } U = 0$$

and

$$\text{at } y = \infty \quad T = T_\infty \text{ and } U = 0$$

By solving equations (5) and (6) with the given boundary conditions, the average value of the convective film coefficient for the entire surface was found to be

$$h = N^4 \sqrt{\frac{g_c p \rho_\infty^2 K^3 (T_s - T_\infty)}{\mu H T_\infty}} \quad (7)$$

Where N is the numerical coefficient, which has been found to be .548 for air at atmospheric pressure.

The average rate of heat transfer by convection from the vertical surface to the surrounding air is

$$q/A = h(T_s - T_\infty) \text{ Btu/ft}^2 \text{ hr.}$$

or

$$q/A = 0.548 \sqrt[4]{\frac{g_c p \rho_\infty^2 K^3}{\mu H T_\infty}} (T_s - T_\infty)^{5/4} \quad (8)$$

Whis is similar to the empirical equation shown below, suggested by Dulong and Petit (2) in 1817 as a result of their experiments.

$$q/A = m \rho^c (T_s - T_\infty)^b \quad (9)$$

For all gases and vapors that have been investigated, the value of b in the equation (9) has been found to be 1.233, in comparison with 1.25 given in equation (8).

Dulong and Petit found the following values for the exponent c :

$$c = .45 \text{ for air}$$

$$c = .315 \text{ for water vapor}$$

$$c = .517 \text{ for carbon dioxide}$$

$$c = .501 \text{ for ethylene}$$

These values are fairly close to the value 0.500 given in equation (7).

The close agreement between these two independent researchers provided a basis for much of the natural convection correlation efforts to be achieved in later years.

Additional experiments with air relating to Lorenz's work were carried out by Nusselt (6) in 1909 and his results indicated that, in the range of excess temperature ($\theta = T_s - T_\infty$) from 0 to 20 F, the Lorenz solution was not applicable, especially as the excess temperature approached zero.

Further experiments on vertical plates were conducted by Griffiths and Davis (3) in 1922, in which the author verified Lorenz's theory that the heat transfer coefficient increases in direct proportion to the fourth root of the plate height for plates three to four feet high. In experiments conducted on plates nine feet high they found neither the velocity nor the temperature increased for measurements

taken beyond 3.6 feet from the lower edge and at a distance of 1/5 inches from the plate. This was hypothesized to be the effect of turbulence, and was observed to occur at a point approximately 1.5 feet from the lower edge.

Experiments similar to those of Griffiths and Davis were conducted by Nusselt and Juerges (6) in 1928, on vertical plates of approximately two feet in length, and their results substantiated those of Griffiths and Davis in the region below the start of turbulence.

Improvements in the analytical theory were attempted by Nusselt and Juerges, but it wasn't until 1930 that E. Schmidt and W. Beckmann (9) made improvements in the theory that provided a more substantial analytical solution to the vertical plate natural convection problem.

Schmidt and Beckmann solved, with the aid of E. Pohlhausen, a modified set of the momentum and energy equations by introducing the stream function and two variables which allowed the resulting equations to be numerically integrated.

Starting with the basic equations involved for a steady state condition:

$$U \frac{\partial U}{\partial x} + V \frac{\partial U}{\partial y} = \nu \left(\frac{\partial^2 U}{\partial x^2} + \frac{\partial^2 U}{\partial y^2} \right) + g \left(\frac{\rho_\infty - \rho}{\rho} \right) \quad (10)$$

$$U \frac{\partial U}{\partial x} + V \frac{\partial U}{\partial y} = \nu \left(\frac{\partial^2 U}{\partial x^2} + \frac{\partial^2 U}{\partial y^2} \right) \quad (11)$$

$$\frac{\partial U}{\partial x} + \frac{\partial V}{\partial y} = 0 \quad (12)$$

$$U \frac{\partial T}{\partial x} + V \frac{\partial T}{\partial y} = \frac{K}{\rho c_p} \left(\frac{\partial^2 T}{\partial x^2} + \frac{\partial^2 T}{\partial y^2} \right) \quad (13)$$

Schmidt and Beckmann chose to consider an incompressible flow with the buoyant effect introduced in the last term of equation (10). Considering a low-pressure isobaric field; the buoyancy term, with the use of the ideal gas relationship, was approximated to be:

$$\frac{\rho_\infty - \rho}{\rho} \approx \frac{T - T_\infty}{T_\infty} \quad (14)$$

Schmidt and Beckmann conducted an order-of-magnitude study which led to the deletion of some of the terms in equations (10) through (13). The deletion of these terms and the logic justifying their removal are shown here.

Since $U \gg V$ for nearly all x (the only deviation here is in the vicinity of the lower edge of the plate); the entire momentum equation in the y direction, equation (11), was eliminated.

Since $\partial T / \partial x < \partial T / \partial y$, then $\partial^2 T / \partial x^2$ was eliminated on the basis that

$$\frac{\partial^2 T}{\partial x^2} \ll \frac{\partial^2 T}{\partial y^2}$$

Similarly, $\partial U/\partial x < \partial U/\partial y$, thus $\partial^2 U/\partial x^2$ was eliminated since

$$\frac{\partial^2 U}{\partial x^2} \ll \frac{\partial^2 U}{\partial y^2}.$$

With these deletions, the system of equations (10) through (13), became

$$U \frac{\partial U}{\partial x} + V \frac{\partial U}{\partial y} = \nu \frac{\partial^2 U}{\partial y^2} + g \left(\frac{T_s - T_\infty}{T_\infty} \right) \theta \quad (15)$$

$$\frac{\partial U}{\partial x} + \frac{\partial V}{\partial y} = 0 \quad (16)$$

$$U \frac{\partial \theta}{\partial x} + V \frac{\partial \theta}{\partial y} = \alpha \frac{\partial^2 \theta}{\partial y^2} \quad (17)$$

where θ (excess temperature) was defined as $\left(\frac{T - T_\infty}{T_s - T_\infty} \right)$.

Introducing the stream function, ψ , where:

$$U = \frac{\partial \psi}{\partial y}$$

and

$$V = - \frac{\partial \psi}{\partial x}$$

Equations (15) and (17) were then written as a function of θ and ψ

$$\frac{\partial \psi}{\partial y} \frac{\partial^2 \psi}{\partial x \partial y} - \frac{\partial \psi}{\partial x} \frac{\partial^2 \psi}{\partial y^2} = \nu \frac{\partial^3 \psi}{\partial y^3} + g \left(\frac{T_s - T_\infty}{T_\infty} \right) \theta \quad (18)$$

$$\frac{\partial \psi}{\partial y} \frac{\partial \theta}{\partial x} - \frac{\partial \psi}{\partial x} \frac{\partial \theta}{\partial y} = \alpha \frac{\partial^2 \theta}{\partial y^2} \quad (19)$$

To solve this system of equations, Pohlhausen defined the similarity parameter:

$$\eta = \sqrt[4]{\frac{(T_s - T_\infty)g}{4\nu^2 T_\infty}} \frac{y}{\sqrt[4]{x}} = c y / \sqrt[4]{x} \quad (20)$$

and the functions θ and ψ were transformed to F and G where:

$$\psi(x, y) = 4\nu c x^{3/4} F(\eta) \quad (21)$$

$$\theta(x, y) = G(x, y) \quad (22)$$

Since the components of velocity, U and V , were related through the stream function and also to the variable η ,

$$U = \frac{\partial \psi}{\partial y} = \frac{\partial \psi}{\partial \eta} \cdot \frac{\partial \eta}{\partial y} = 4\nu c x^{3/4} F'(\eta)$$

$$\begin{aligned} V &= -\frac{\partial \psi}{\partial x} = -\frac{\partial}{\partial x} (4\nu c x^{3/4} F(\eta)) \\ &= c\nu x^{-1/4} (\eta F'(\eta) - 3F(\eta)) \end{aligned}$$

and similarly:

$$\begin{aligned}\frac{\partial U}{\partial x} &= \frac{\partial}{\partial x} \left(\frac{\partial \psi}{\partial y} \right) = \frac{\partial}{\partial x} [4\nu C x^{2/4} F'] \\ &= \nu C x^{-2/4} [2F' - \eta F'']\end{aligned}$$

$$\frac{\partial U}{\partial y} = \frac{\partial}{\partial y} \left(\frac{\partial \psi}{\partial y} \right) = 4\nu C x^{3/4} F''$$

Accomplishing all necessary operations and substituting into equations (18) and (19), the final equations become:

$$F''' + 3FF'' - 2(F')^2 + G = 0 \quad (23)$$

$$G'' + \frac{3\nu}{a} FG' = 0 \quad (24)$$

where the primed values are successive derivatives with respect to η . The introduction of η as the only independent variable transformed the original partial differential equations to a simple system of two ordinary differential equations, in F and G , which were solvable by numerical integration.

The transformed boundary conditions were

$$\text{for } \eta = 0 \quad F = 0, \quad F' = 0 \quad G = 1$$

$$\text{and at } \eta = \infty \quad F' = 0 \quad F'' = 0 \quad G = 0$$

Pohlhausen performed a numerical integration using a series expansions for F and G and using values of F'' and G' which were determined experimentally. A plot of the G , G' , F , F' and F'' terms of differential equations (23) and (24) are shown in Figure 3.

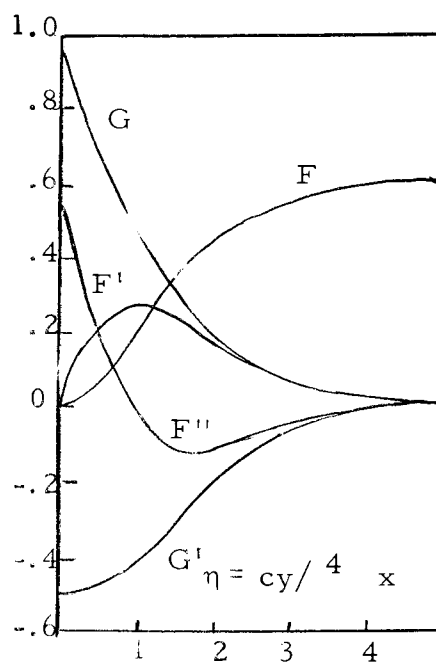


Figure 3. Solution of differential equations (23) and (24) for $Pr = 0.733$ (from Schmidt and Beckmann (9)).

The difference between the Schmidt-Beckmann analysis and those attempted previously (Lorenz, Nusselt-Juerges) lies primarily in the assumed form of the simplified momentum equation. Recall that in equation (5), both the $U(\partial U/\partial x)$ and $V(\partial U/\partial y)$ terms were deleted. These terms were not eliminated from the Schmidt and Beckmann analysis and, in accordance with the test data obtained by Schmidt-Beckmann, this more-inclusive analysis was verified.

An evaluation of the average convective heat transfer coefficient

$$h = N \frac{K}{H} \sqrt[4]{\frac{gH^3(T_s - T_\infty)}{\nu^2 T_\infty}} \quad (25)$$

yielded a value of $N = .479$ whereas Lorenz obtained a value of .507.

Experiments performed by R. Weis (12) 1935, produced results which were some 25 percent higher than the average heat transfer coefficient calculated by Schmidt and Beckmann. It is believed that the experimental set up for both Lorenz and Weise was subject to disturbances which may have caused a significant error in their readings. Analysis beyond the Schmidt and Beckmann solution was not attempted until 1953, when Ostrach (7, 8) performed an analytical study to determine the conditions under which the simplified equations (10) and (13) were significantly accurate to describe a physical case. In his analysis, Ostrach started with the complete set of momentum and energy equations but introduced three variables

in the form:

$$d\rho = \rho(KdT - \beta dT)$$

$$\mu = \mu \left(\frac{T}{T_{\infty}}\right)^m$$

$$K = K \left(\frac{T}{T_{\infty}}\right)^n$$

He concluded that the modified equations represented the physical case adequately, provided that the temperature difference was small, thus resulting in relatively low Grashof numbers. For high Grashof numbers, Ostrach concluded that Nusselt numbers comparable to those in forced convection could be obtained. Velocity and temperature profiles for Prandtl numbers of .01, .72, .733, 1, 2, 10, 100 and 1000 were computed with the aid of L. U. Albers (1), on the basis of a constant body force and plate temperature. Ostrach's analysis agreed very well with the Schmidt and Beckmann velocity experiment data $\eta < 1$ and for all Schmidt and Beckmann temperature data taken on small plates. A comparison of the average heat transfer coefficient obtained by Ostrach in the form of equation (25) gave $N = .505$, a value nearly identical to that obtained by Lorenz. The work of Sparrow and Gregg (10) in 1956, provided a solution of the modified equations for conditions other than an isothermal vertical plate. Specifically, their analysis considered a plate which dissipated heat at a uniform rate q over its entire

surface. For their case, the following boundary conditions applied:

$$\begin{aligned} \text{at } y = 0 \quad U = V = 0 \quad \frac{\partial T}{\partial x} = \text{constant} \\ y = \infty \quad U = 0 \quad T = T_{\infty} \end{aligned} \quad (26)$$

To satisfy the preceding boundary conditions, the temperature variable, the generalized stream function and the similarity variable were required to be slightly different than those utilized by Schmidt and Beckmann. The newer forms were

$$\eta = c_1 \frac{y}{\sqrt[4]{x}},$$

$$F(\eta) = \frac{\psi}{c_2 x^{4/5}},$$

The resulting differential equations became:

$$F''' - 3(F')^2 + 4FF'' - G = 0 \quad (27)$$

$$G'' + P_r 4G'F - GF' = 0 \quad (28)$$

Equations (27) and (28) were comparable to the Schmidt-Beckmann equations (23 and 24). Sparrow and Gregg calculated heat transfer parameters resulting from the solution of equations (27) and (28) for Prandtl numbers of .1, 1, 10 and 100. The uniform flux case was found to compare well with Ostrach's solution for the isothermal case suggesting that a single heat transfer relation may

apply accurately for a number of different physical situations.

Sparrow and Gregg (10) also studied the problem using variant and non-variant fluid properties and concluded that, for the property variations typical for gases, the properties other than β should be evaluated at the following reference temperature for vertical isothermal plates with laminar boundary layers:

$$T_f = T_s - .38(T_s - T_\infty) \quad (29)$$

They stated that the expression (29) was valid over the range of

$$.5 < \frac{T_s}{T_\infty} < 3.0$$

where temperatures are expressed in absolute units.

All of this discussion deals with a single vertical plate and an adjacent fluid of infinite extent.

The present study considers two parallel vertical plates with a fluid between them. While this case is governed by the same basic equations as the single plate case the boundary conditions and, hence, the solution is more complex and has not yet been obtained analytically.

DISCUSSION OF APPARATUS AND TEST

General

The factors affecting radiation in a confined air space are the emissivity of the surface and their temperatures; those affecting diffusion are height and width of the spaces and the conductivity of the enclosed fluid. The small temperature difference between plates allowed the radiation effect to be safely neglected.

Therefore an aluminum plate which has high thermal conductivity and low emissivity, and plexiglass which has low thermal conductivity were used for the hot and adiabatic plates respectively in this work.

In order to maintain the surface temperature of the hot plate constant condensing acetone, vaporized by a heating element which was immersed in liquid acetone at the bottom of the assembly, was used. Also the magnitude of the isothermal surface temperature could be altered by varying the condensing temperature with the pressure within the acetone vapor chamber.

In this test the condensing temperature at near atmospheric pressure was used. The temperature difference, 54 F, between the surface at 128 F and the surrounding air at 74 F, was used, this provided circulation within the moderate laminar range.

In measuring the velocity of the air between the plates, a quartz

fiber of the type used by Schmidt was utilized. Calibration of the quartz fiber designed by the author was made.

In measuring the temperature of the air between the plates, an iron-constantan thermocouple was used.

All parts except the hot plate surface and the insulated plate were insulated with fiber-glass so that there was no heat transfer from the acetone chamber to the ambient air.

The air which was initially inside the acetone chamber was gradually evacuated by a water-aspirator connected to the upper portion of the chamber while the liquid acetone was added and heated.

Acetone vapor replaced the air removed by the aspirator. After about five hours elapsed time the acetone chamber contained very little air and was occupied by essentially 100 percent acetone.

Positioning of the Vertical Plates

Both plates were first adjusted by screws in the supporting structure to get the desired distance between them and to align them to be both vertical and parallel. The distance between the plates was accurately measured by a micrometer at a number of positions. The vertical positioning was obtained by means of a plumb line.

The bottom edges of the plates were positioned three feet away from the ground. The position of these plates is shown in Figure 4.

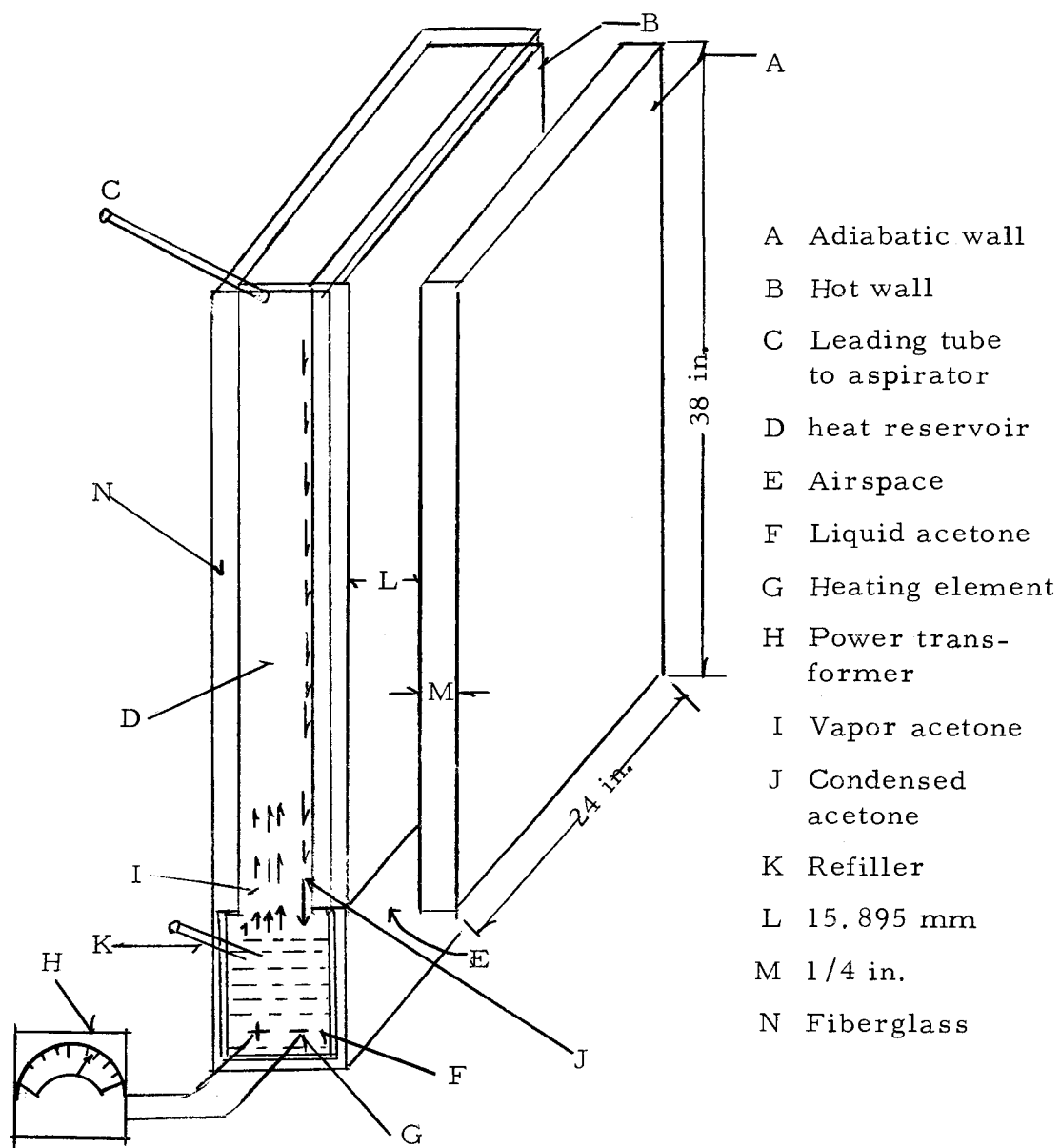


Figure 4. Scheme of two vertical plates.

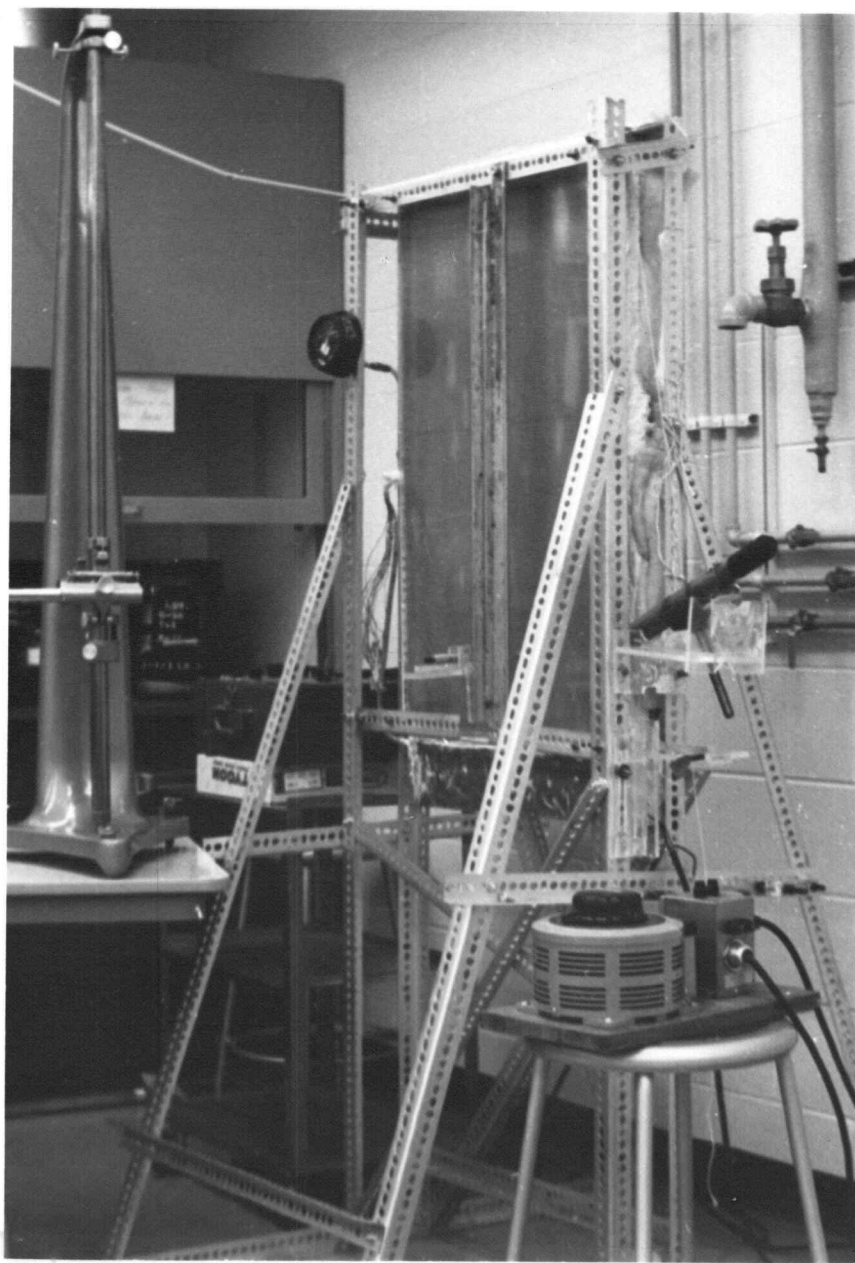


Figure 5. Whole view of apparatus.

Hot Plate Assembly

The hot plate was made of $1/4$ in. thick, 24 in. wide, 38 in. high aluminum plate. Provisions were made for inserting 15 thermocouples into the plate for surface temperature measurements. The thermocouple holes in the plate were drilled $1/16$ in. in diameter and their exact locations and depths are shown in Figure 6. Liquid aluminum was used to fix each thermocouple junction point in a hole, and the thermocouple leads were attached to a Millivolt Potentiometer.

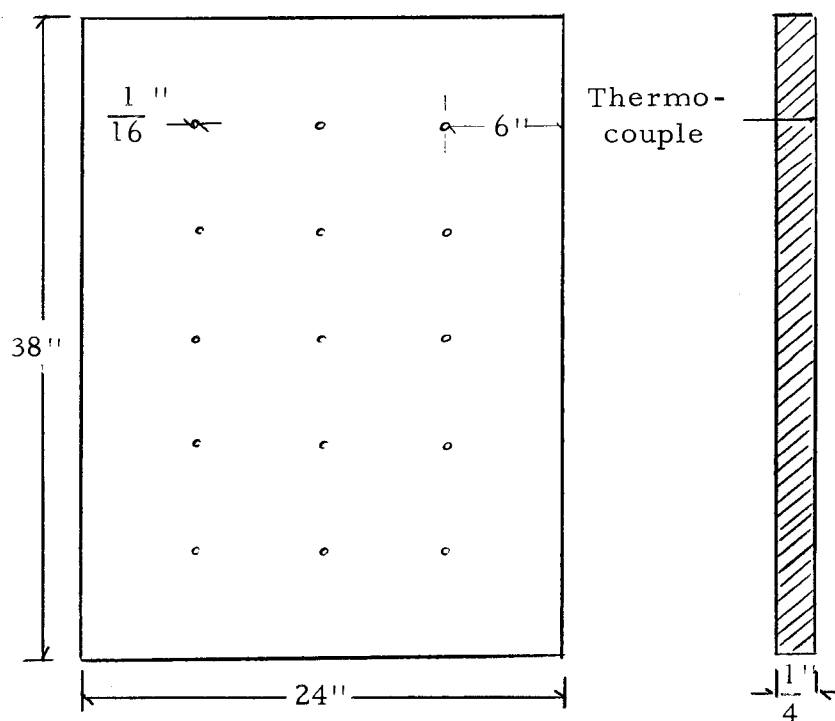


Figure 6. Positions of thermocouples on hot plate.

The plate was heated to a constant temperature by condensing acetone. A typical temperature distribution for the plate is shown in Figure 7. The maximum temperature variation from bottom to top was 1.6 F or an average gradient of .042 F/in. Five to six hours were required to get the surface temperature to this nearly uniform condition; the proper power input to the heating element was obtained by trial and error.

Adiabatic Plate Assembly

The adiabatic surface consisted of $1/4 \times 24 \times 38$ in. Plexiglass. The temperature gradient was assumed zero because of the relatively low thermal conductivity of this material. In the velocity measurements the deflection of the quartz fiber was observed by viewing through this plate. In order to measure the distances between the quartz fiber and the wall, holes of $1/32$ in. in diameter were drilled through the plexiglass and a thin wire connected to a micrometer inserted into them. As the position of the quartz fiber was changed it was optically aligned parallel to the plates by a telescope and its position between the plates was determined from the micrometer arrangement discussed above.

Heat Reservoir

In order to maintain the hot plate at a uniform temperature the

Reference
 Temperature 74 F
 Pressure 14.148 psi
 Power State $60/100 \times 140 = 84$ volts
 Contents Acetone

—△—△—△

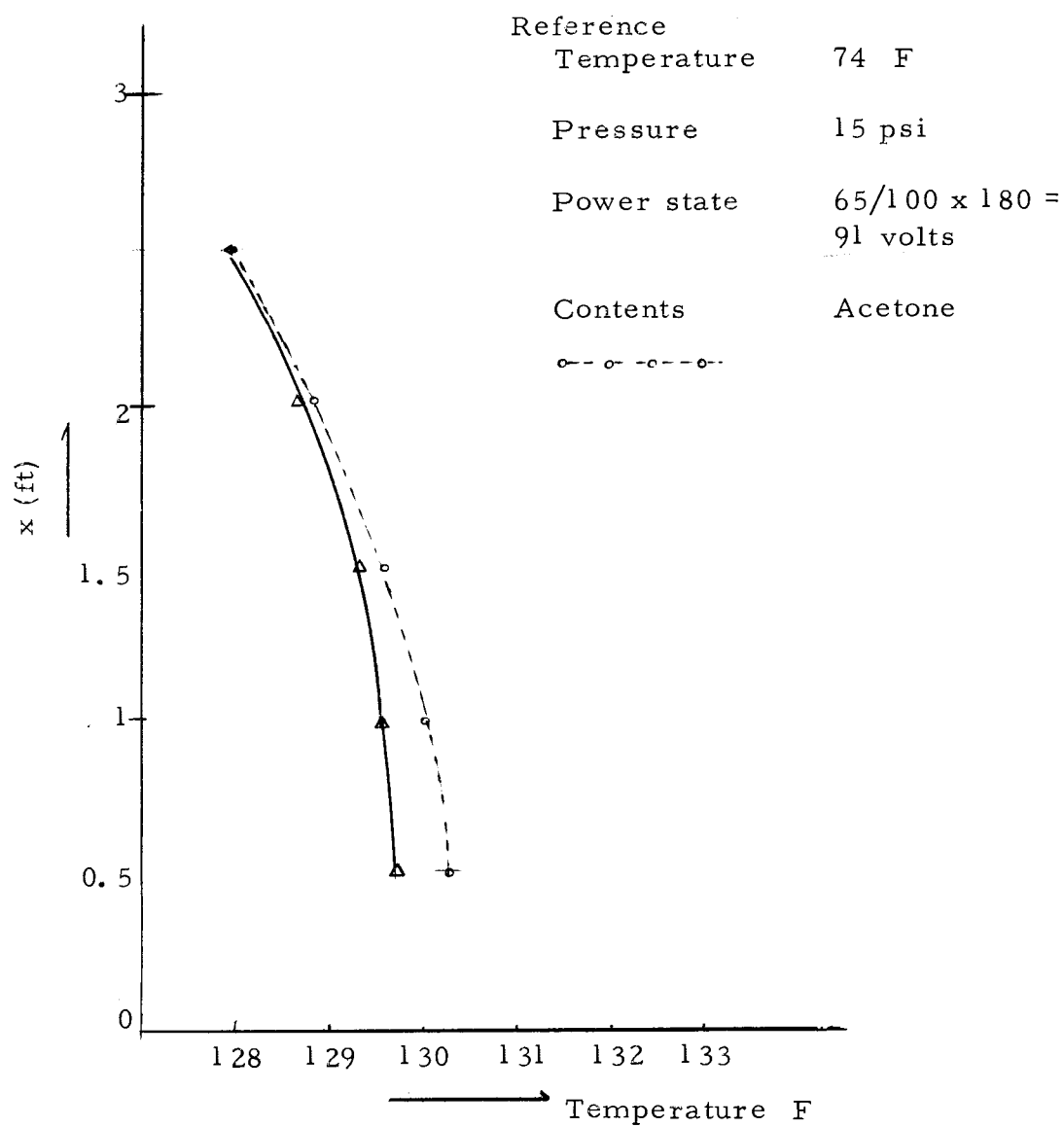


Figure 7. Local temperatures on the hot surface.

liquid acetone was heated and vaporized by the heating element immersed in liquid acetone at the bottom of the assembly.

Power Level

The proper power level to the acetone was obtained by varying the setting on a variable transformer. This was a trial and error process.

Pressure Measurement

A manometer was used for accurate pressure control of the acetone chamber after steady-state operation was established. The range of the pressure measurement was ± 7 inches of water.

Millivolt Potentiometer

A Leeds and Northrup model 8686 portable potentiometer was used to measure the surface temperature of the hot plate. Cold-junction compensation was used to adjust the reference junction temperature to 32 F.

Aspirator

The air from inside the acetone chamber was slowly evacuated while the liquid acetone was vaporized and its volume expanded. A water aspirator was used for this evacuation, which was convenient

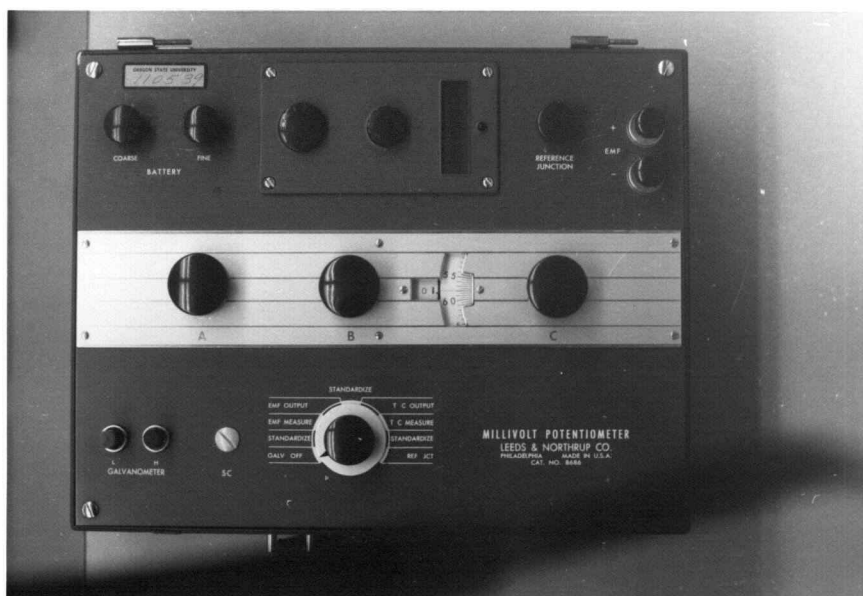


Figure 8. Millivolt potentiometer, top view.

for controlling the vacuum pressure by simply adjusting the flow rate of water.

The aspirator was connected to the upper portion of the acetone chamber.

Calibration of the Velocity Measuring Instrument

The method of measuring air velocities between the hot plate and the adiabatic plate was to observe the deflection of a quartz fiber, .015 mm diameter and 13 mm long.

The deflection of the quartz fiber due to the influence of the flow, which can be considered a measurement of the local air velocity, was observed by a microscope. This is the same method used by Schmidt and Beckmann in 1930. The range of air velocities in free convection was so low that it was impossible to measure by other means.

Calibration of the quartz fiber was accomplished using the apparatus shown in Figure 9. Considerable care and precision were necessary for accurate calibration of this device. Various conditions which were found to influence velocity readings included building air conditioning and air currents induced by opening and closing the laboratory door.

Items of apparatus include the following:

1. Air pump. This pump could control to a minimum flow rate

A Wet test precision flow meter

B Blowing pump

C Circular pipe

D Quartz fiber thread

E Rectangular duct

F Rod

G Telescope

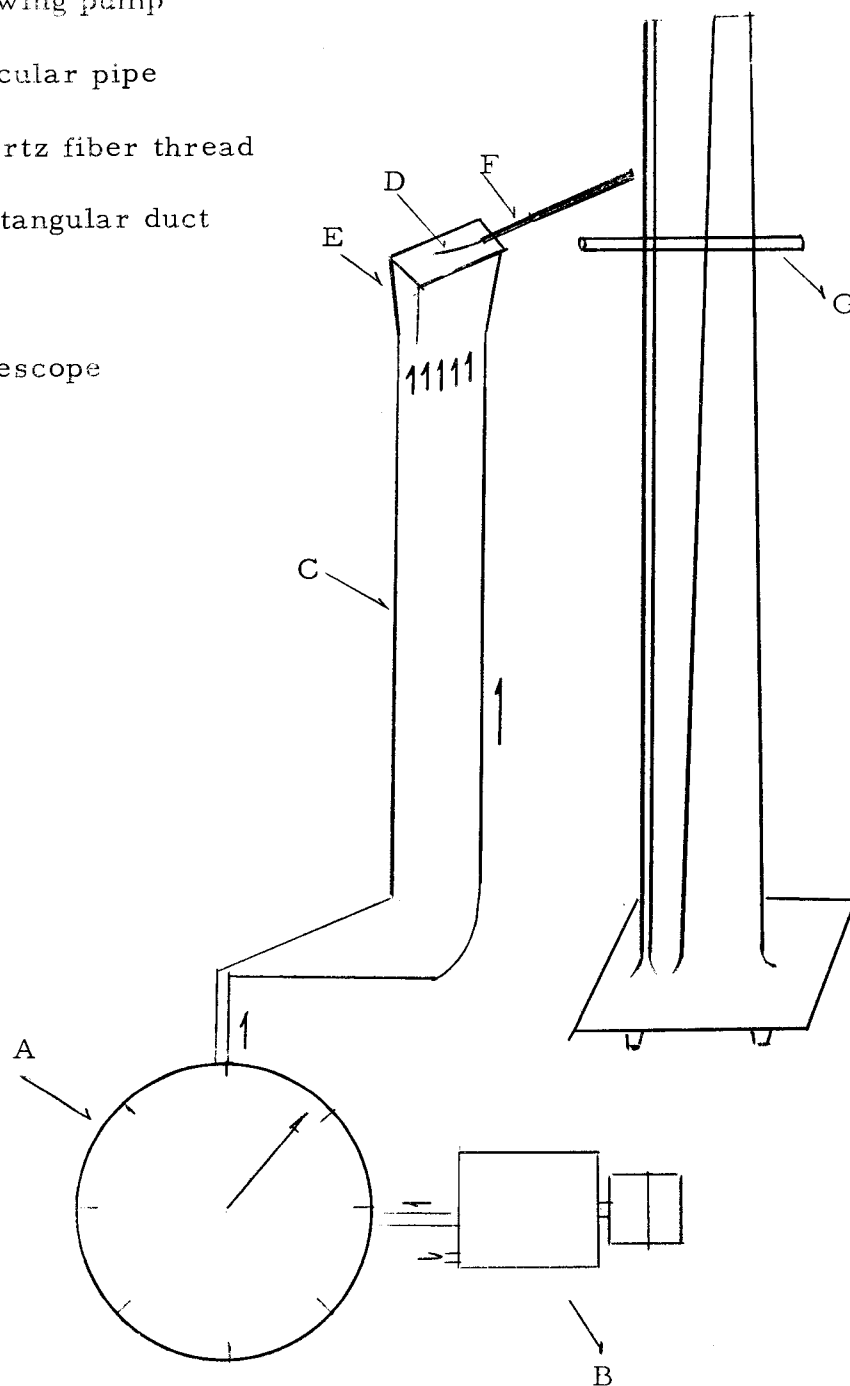


Figure 9. Scheme of calibration apparatus of quartz fiber.

of 1 cfh. It was possible to decrease the flow rate still further but the precision was lost for these lower rates.

2. West test precision flow meter. This meter was connected to the air pump and a flow rate measured for one minute. The minimum flow rate used was $.01 \text{ ft}^3/\text{minute}$ which was sufficient for this work, however, the maximum flow rate available was $1.16 \text{ ft}^3/\text{minute}$.

The velocity at the outlet of the flow meter was still higher than the expected air velocity due to natural convection; therefore, in order to reduce the air velocity a plastic pipe with flow area 1283 times the outlet area of the flow meter was connected to it. With this plastic pipe the smallest velocity at the outlet of the flow meter, 295 cm/sec was reduced to $.23 \text{ cm/sec}$ at the pipe exit. For the low velocities a four square-inch exit area was used, and for the higher velocities the exit area was reduced to two square inches. A rectangular flow passage was connected to the top of the circular plastic pipe to obtain a nearly uniform velocity profile.

Measurement of the air velocity was obtained by using a quartz fiber which was deflected due to the influence of air flow; the minimum velocity that could be read by this device with reasonable certainty was $.6 \text{ cm/sec}$. If a finer fiber and more powerful telescope were used, a lower limit of $.5 \text{ mm/sec}$ is possible. The fiber remained surprisingly steady in the air stream. A drawing of the

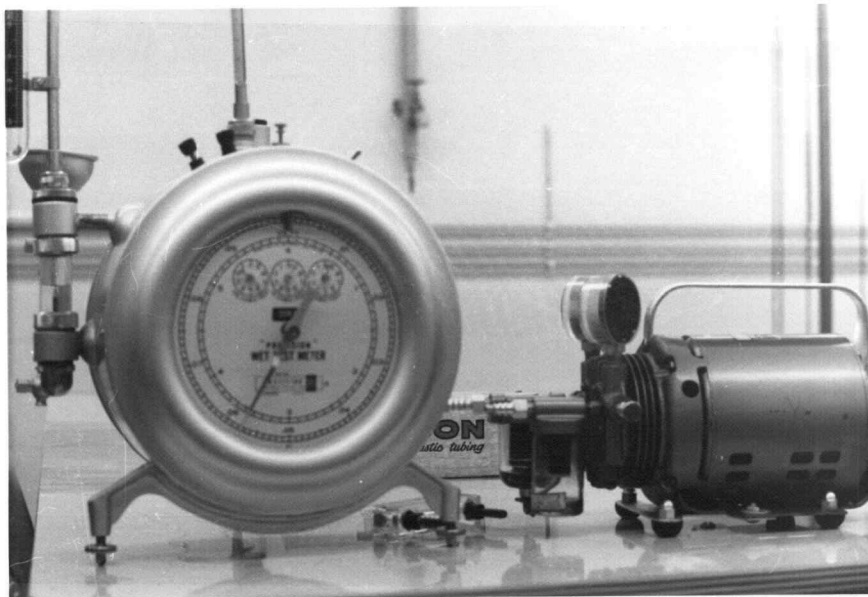


Figure 10. Wet test precision meter and air pump.

quartz fiber is shown in Figure 11.

The deflection data corresponding to known velocities were obtained from the telescope readings. The calibration data appear in Table 1 (Appendix) and are plotted in Figure 12.

It is interesting to note that the velocity is not directly proportional to the deflection of the quartz fiber.

Dimension of quartz fiber: length: 13 mm
 diameter: .015 mm

- A Aluminum square bar
- B Steel rod
- C Quartz fiber

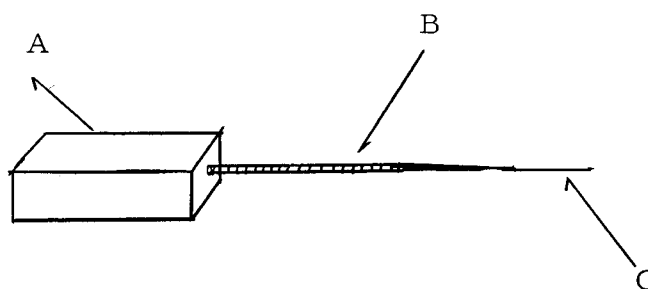


Figure 11. Scheme of quartz fiber.

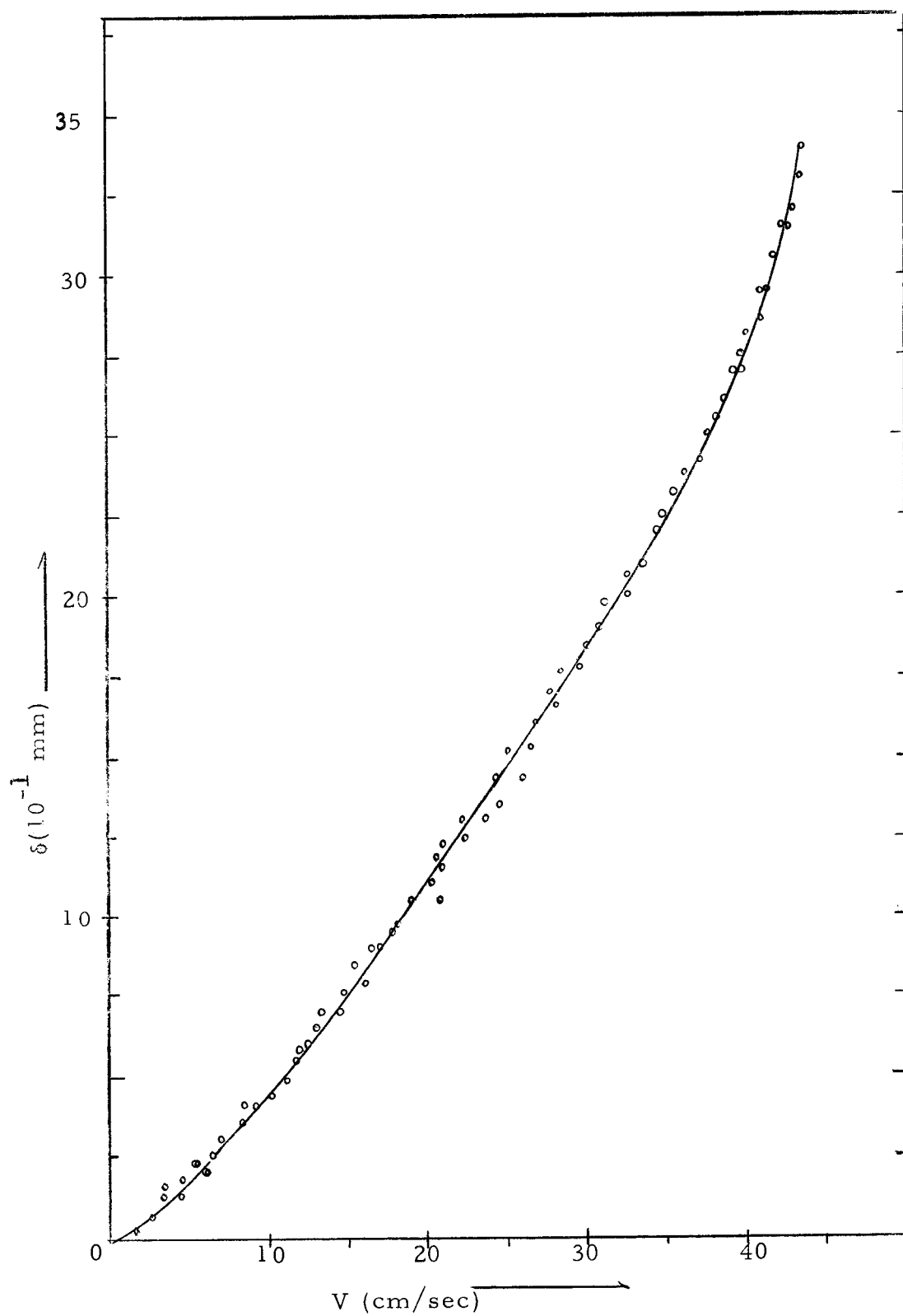


Figure 12. Graph of quartz fiber calibration.

RESULTS AND CONCLUSIONS

Velocity Measurements

The difficulty in measuring low velocities were overcome by using the quartz fiber anemometer designed by the author, and previously discussed.

The dimensionless air velocity U/U_{ave} along the vertical plates is plotted in Figure 13. Most of the velocity profiles obtained were as expected from the results of similar studies; however, those obtained very near the entrance ($x = .25$ in. and $x = .5$ in.) were not as expected; their different appearance are to be noted in Figure 13. A possible explanation for the appearance of the velocity profiles near the bottom of the plates is that, in this region, entrance effects are significant; additionally any air currents in the laboratory will affect the velocity profiles in this region as well.

In Figure 13, it appears that, for $.3 < y/L < .7$, the velocity profiles are very flat. It appears that flow becomes turbulent beyond $x = 20$ in. ($x/H = .528$).

The average velocities across the total width of air space, L , were obtained by integrating the velocity between the limits $y = 0$ and $y = L$ and dividing by L according to

$$U_{ave} = 1/L \int_0^L U dy \quad (30)$$

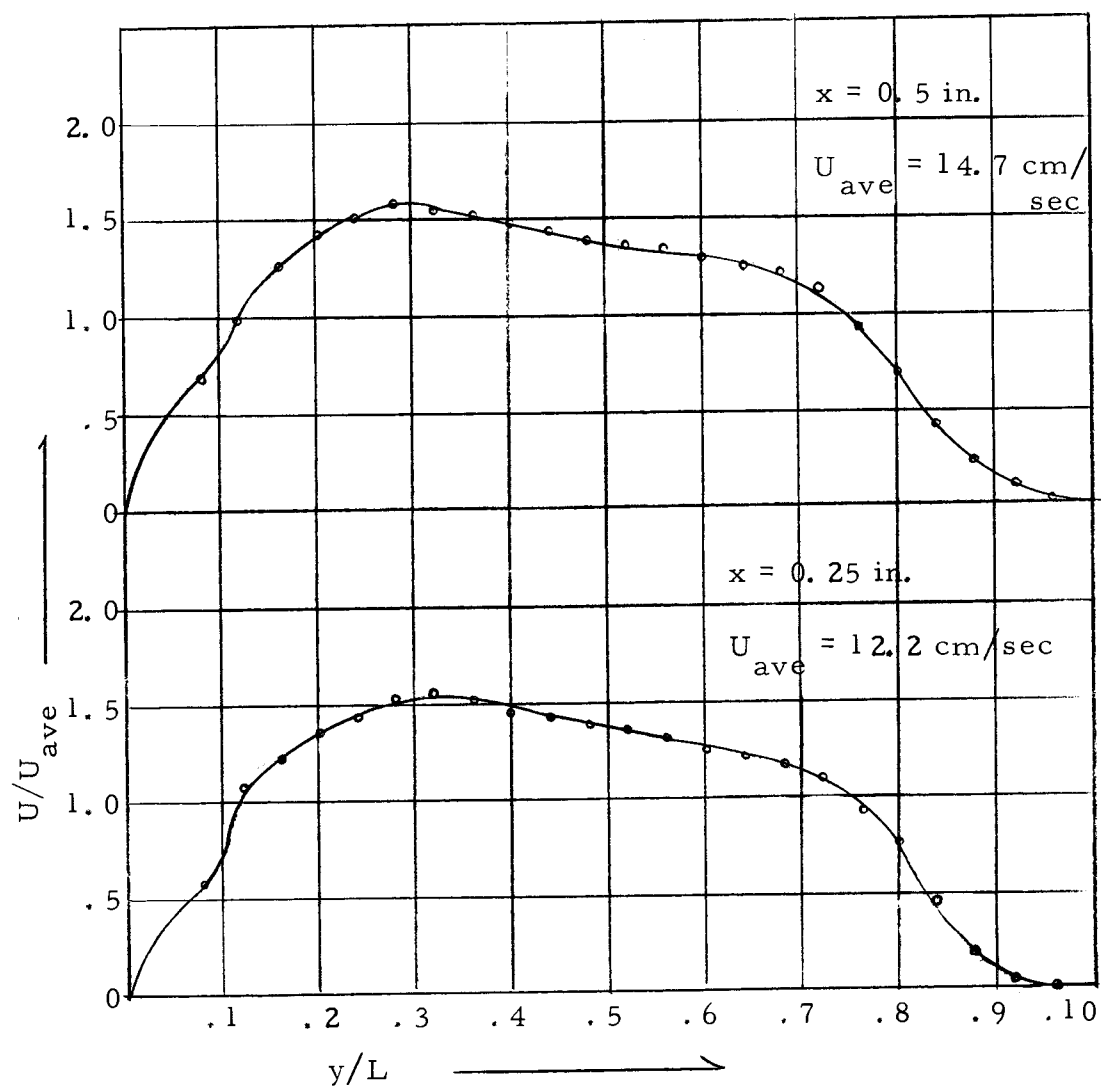


Figure 13. Dimensionless velocity profiles.

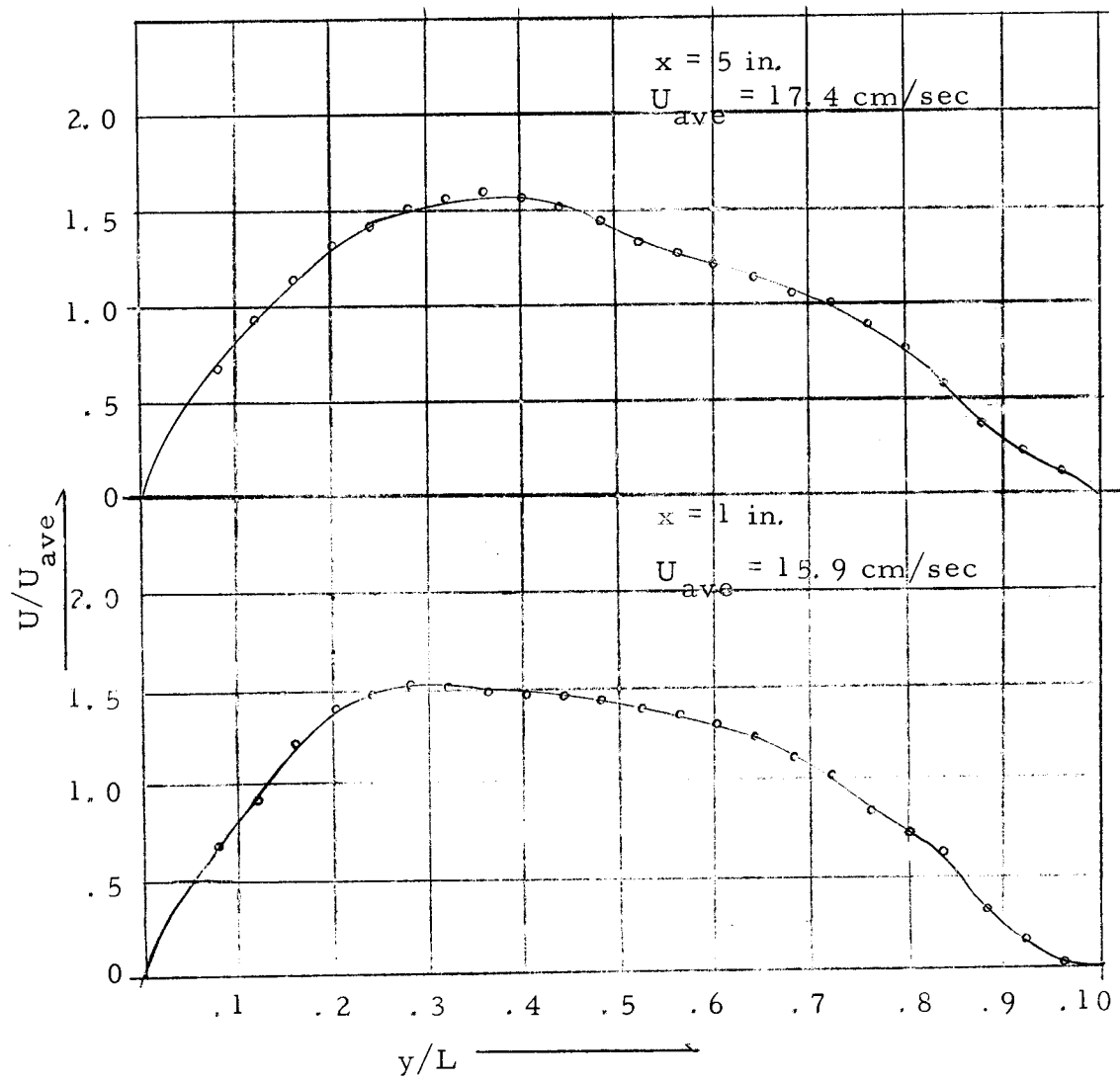


Figure 13. Continued.

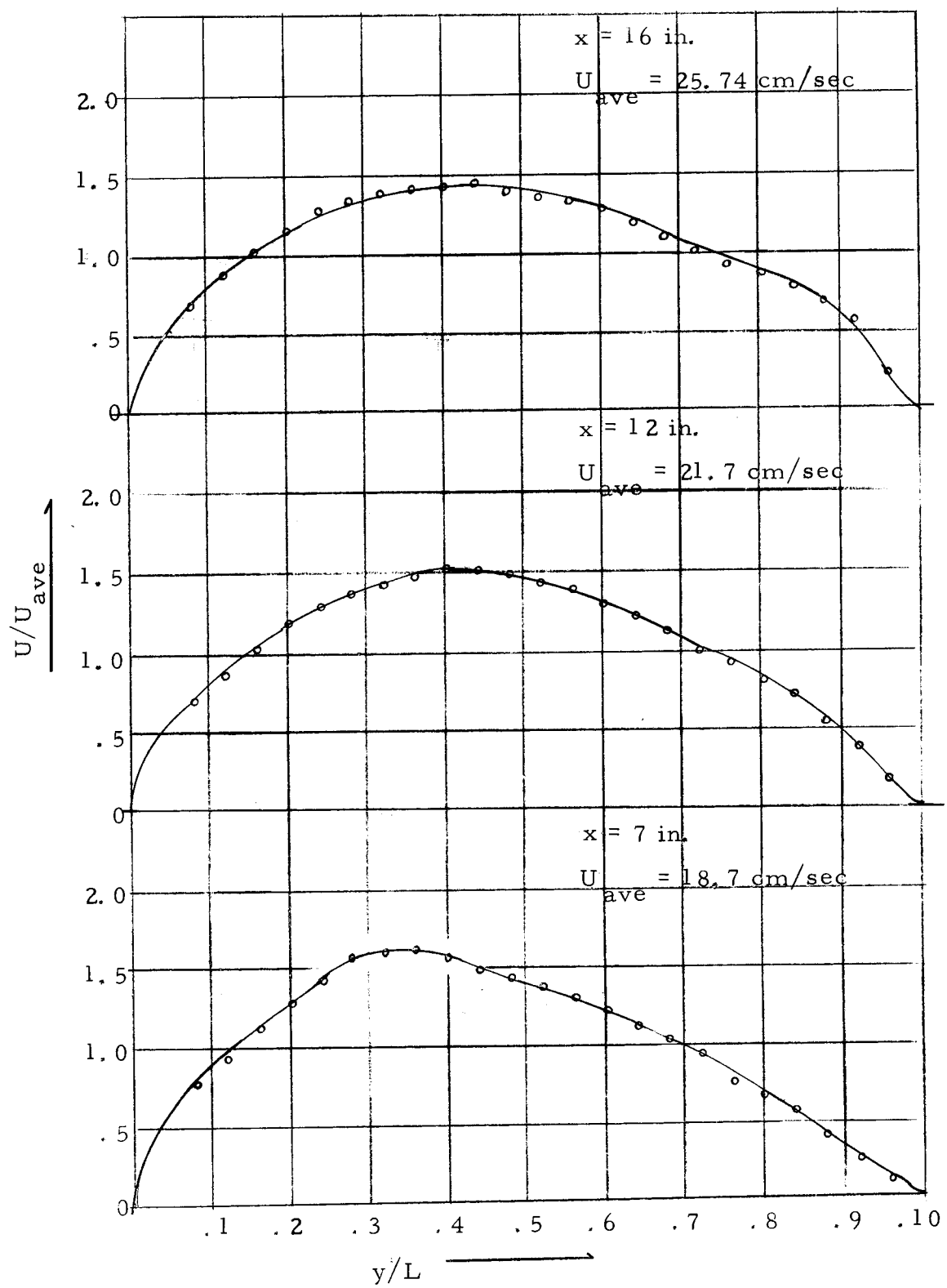


Figure 13. Continued.

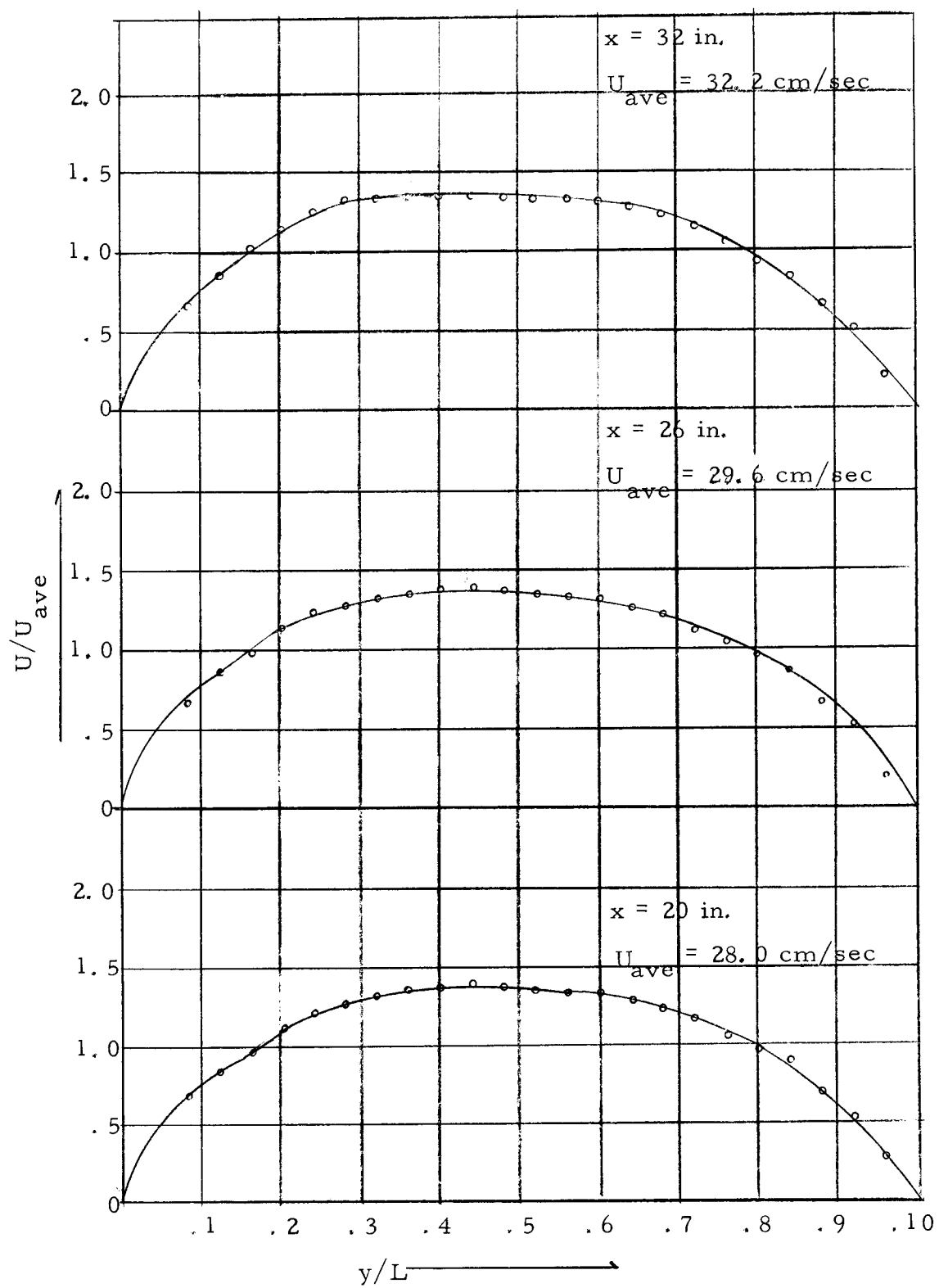


Figure 13. Continued.

Temperature Measurements

The author tried to use a hot-wire anemometer for the temperature measurements in the air between the vertical plates, but this device was not adequate since the air velocities were extremely low. Therefore, an iron-constantan thermocouple, with wire diameters of 0.1 mm and a hot-junction diameter of 0.46 mm, was used for temperature measurements. The lead wires to the thermocouple were connected to the Millivolt Potentiometer.

The distances between the hot-junction of the thermocouple and the hot plate were measured by the micrometer and were checked by observations made through the telescope in the same way as was done for the velocity measurements.

During the test, the room temperature, which was the reference temperature of the Millivolt Potentiometer was observed to account for any change. No such changes were observed at any time.

It took very few seconds to reach steady state at the junction of the thermocouple due to its small size and high conductivity.

The temperature profiles obtained in air at various distances from the lower edge of the vertical plates are shown in Figure 14.

The dimensionless temperatures, $\theta = (T_s - T_f) / (T_s - T_{ave})$, for air flow along the vertical plates are given in Table 3, (Appendix) and are plotted in Figure 15. The average temperatures for the air

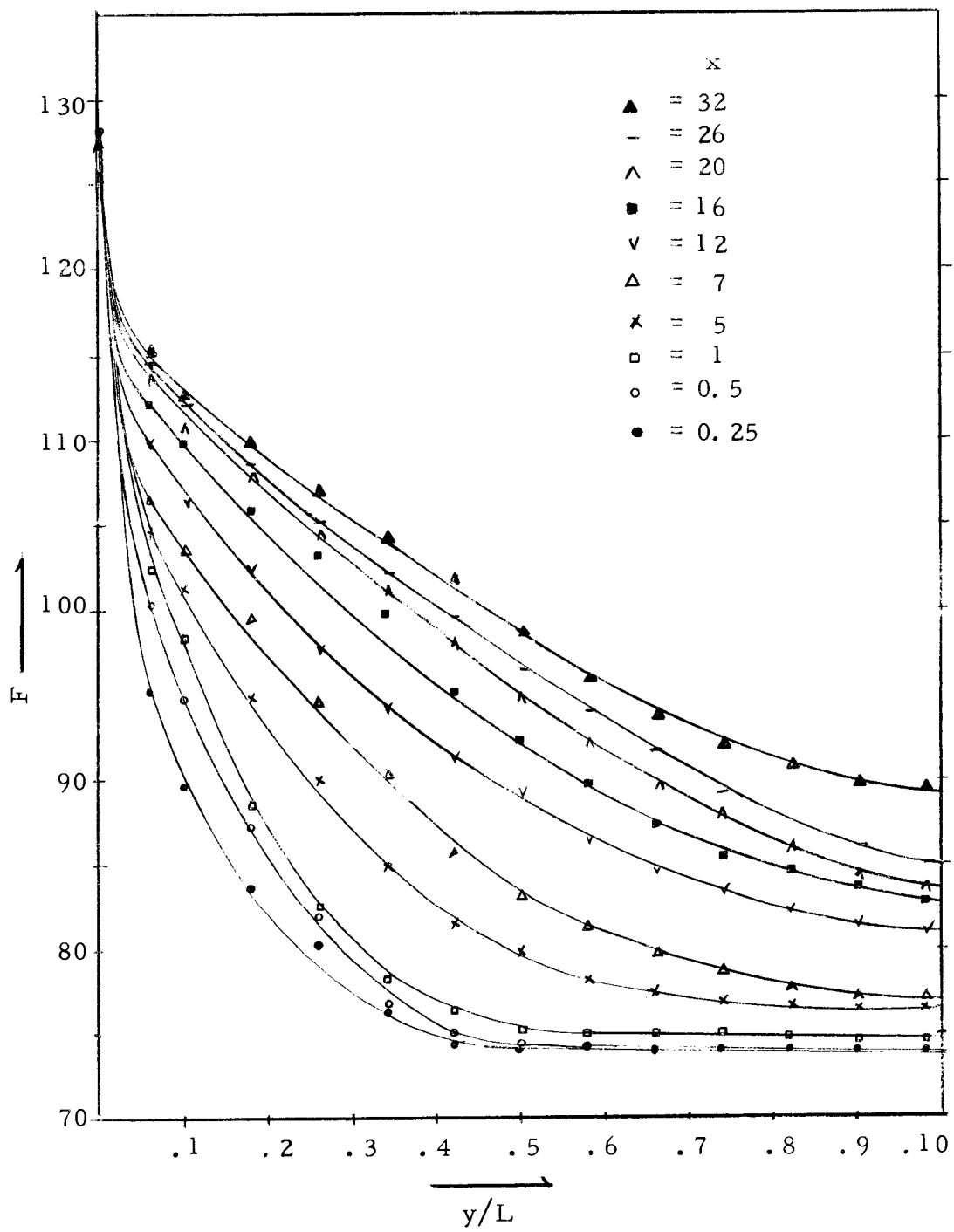


Figure 14. Temperature profiles.

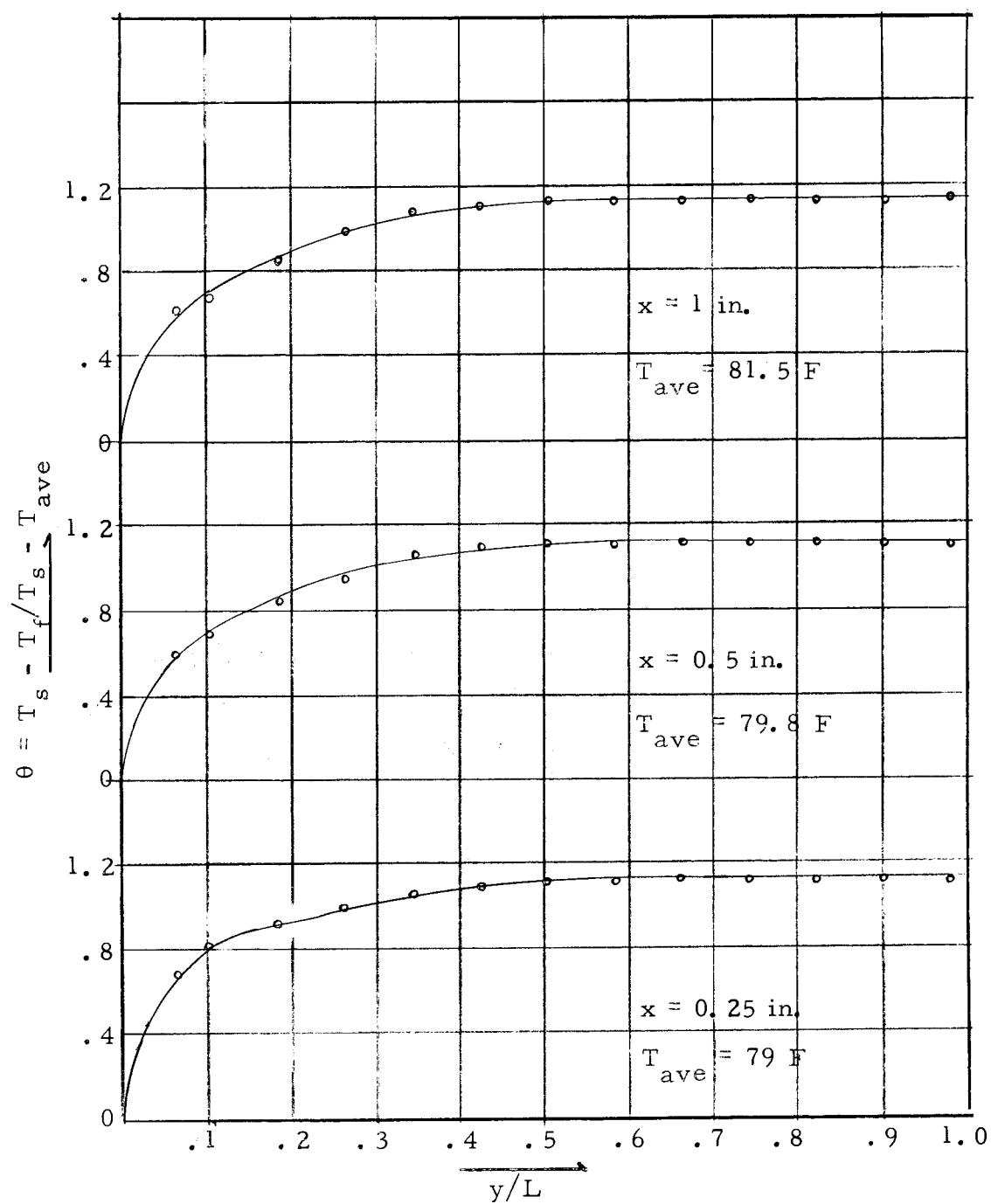


Figure 15. Dimensionless temperature profiles.

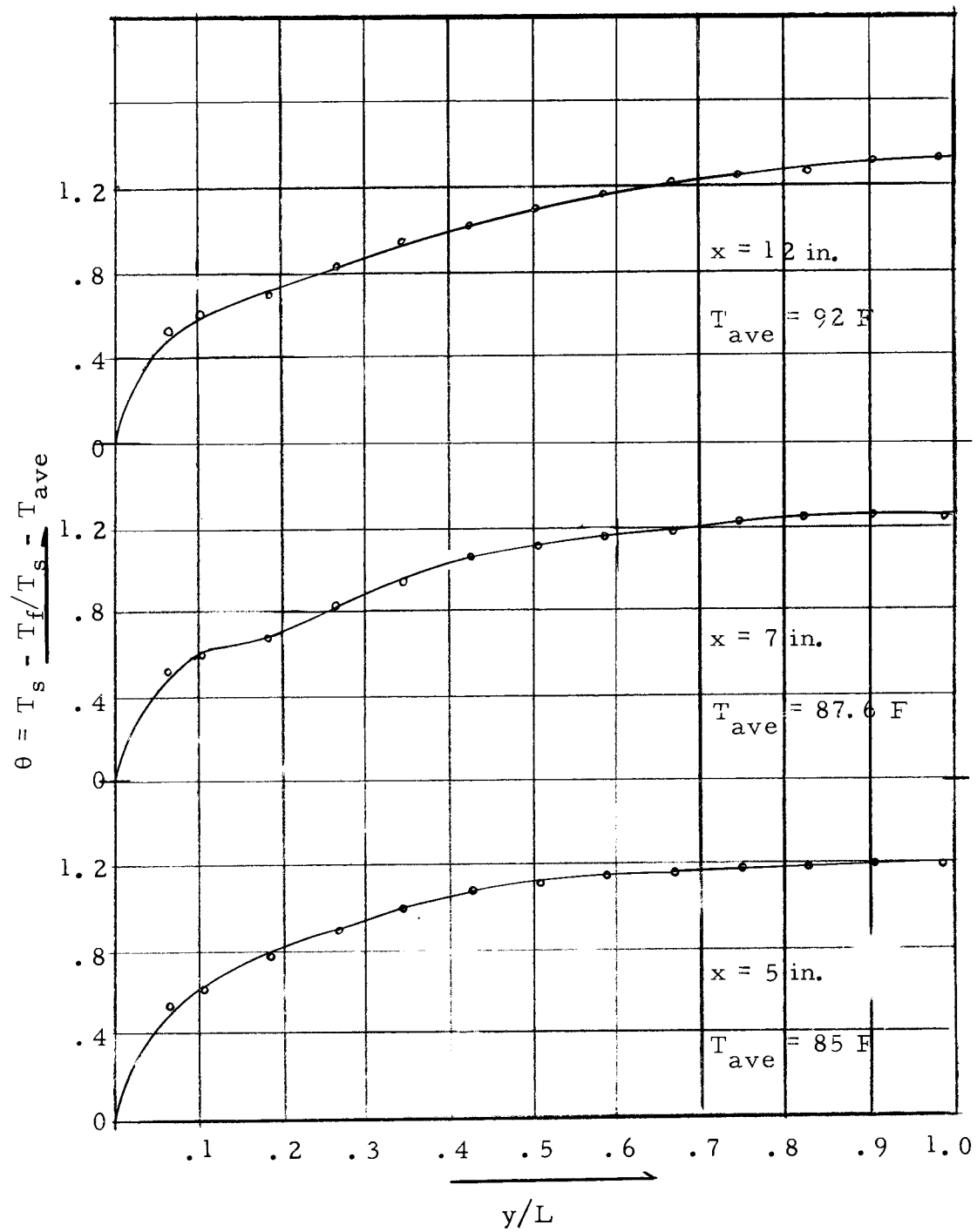


Figure 15. Continued.

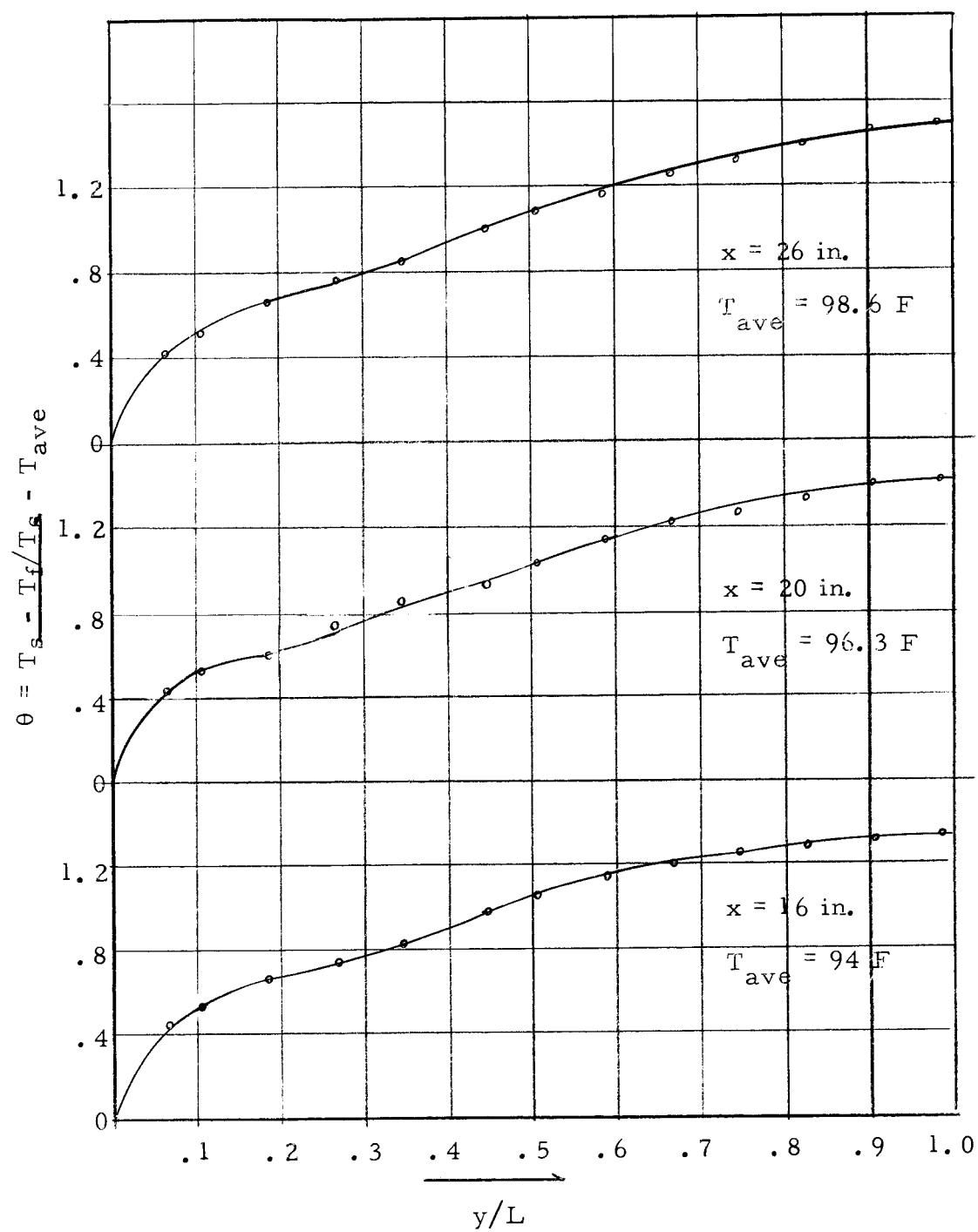


Figure 15. Continued.

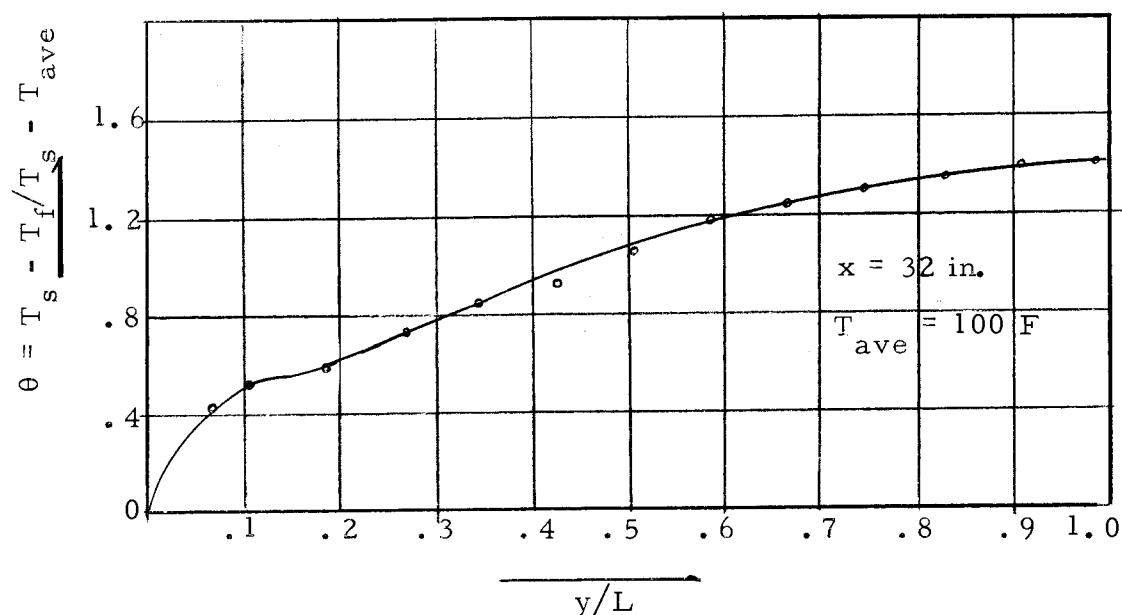


Figure 15. Continued.

space of width L were obtained by integrating between the limits $y = 0$ and $y = L$ and dividing by L as given by

$$T_{ave} = \frac{1}{L} \int_0^L T_f dy \quad (30-1)$$

The characteristic dimension is attached as a suffix to the dimensionless parameters Nu and Gr . All physical properties for air were evaluated at 100 F, which was very near the average temperature throughout the entire length of flow passage.

It may be seen that the temperature gradients are largest near the leading edge and become smaller with increasing distances from the bottom.

The average Nusselt numbers along the vertical plates were

calculated as follows

$$q/A = -K \frac{dT}{dy} \bigg|_{y=0} = h_L (T_s - T_{ave}) \quad (31)$$

Substituting the dimensionless quantities into equation (31)

$$\begin{aligned} q/A &= -K \frac{1}{K} \frac{d\left(\frac{T_s - T_f}{T_s - T_{ave}}\right)}{d(y/L)} \bigg|_{y=0} \\ &= \frac{h_L L}{K} \end{aligned} \quad (32)$$

where the Nusselt number $(N_{Nu})_L$ is based on the thickness of the air layer, L

$$\begin{aligned} (N_{Nu})_L &= \frac{h_L L}{K} \\ &= -L \frac{d\theta}{dy} \bigg|_{y=0} \end{aligned}$$

and

$$\theta = \frac{T_s - T_f}{T_s - T_{ave}}$$

The temperature gradients at the wall,

$$\frac{d\theta}{d\left(\frac{y}{L}\right)} \bigg|_{y=0}$$

were obtained from the temperature profiles and $(N_{Nu})_L$ was determined graphically as shown in Figure 16. The Nusselt numbers calculated are plotted in Figure 17. The Nusselt number profiles near the bottom of the plates are very steep when compared to those at larger values of x indicating a definite edge effect.

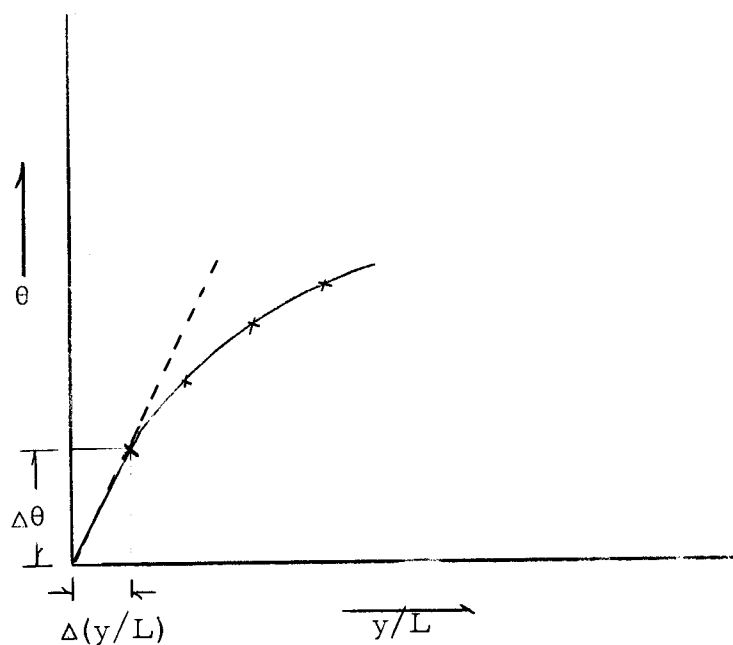


Figure 16. Graphical determination of $\frac{d\theta}{d(y/L)}_{y=0}$.

In Figure 17, the Nusselt numbers beyond $x = 20$ in. are almost constant, thus they do not vary with the ratio H/L . It is very likely that the effect of the height of the vertical plates becomes more pronounced as its value decreases.

The Nusselt number plotted as a function of Grashof number is shown in Figure 18.

Mean values of the Nusselt number for a given surface are identified by a bar, $(\overline{N_{Nu}})_L$; they were calculated as follows

$$(\overline{N_{Nu}})_L = \frac{1}{H} \int_0^H (N_{Nu})_L dx$$

where $(N_{Nu})_L$ is the local Nusselt number along the vertical plates. Simpson's rule was used for this numerical integration.

The mean value for unit surface conductance for a given surface is identified by a bar, (\overline{h}) and is calculated by

$$(\overline{N_{Nu}})_L = \frac{\overline{h}L}{K}$$

$$\overline{h} = \frac{K}{L} (\overline{N_{Nu}})_L$$

In order to get the total heat transfer rate from the hot plate the total mean temperature must be known. It is determined as follows

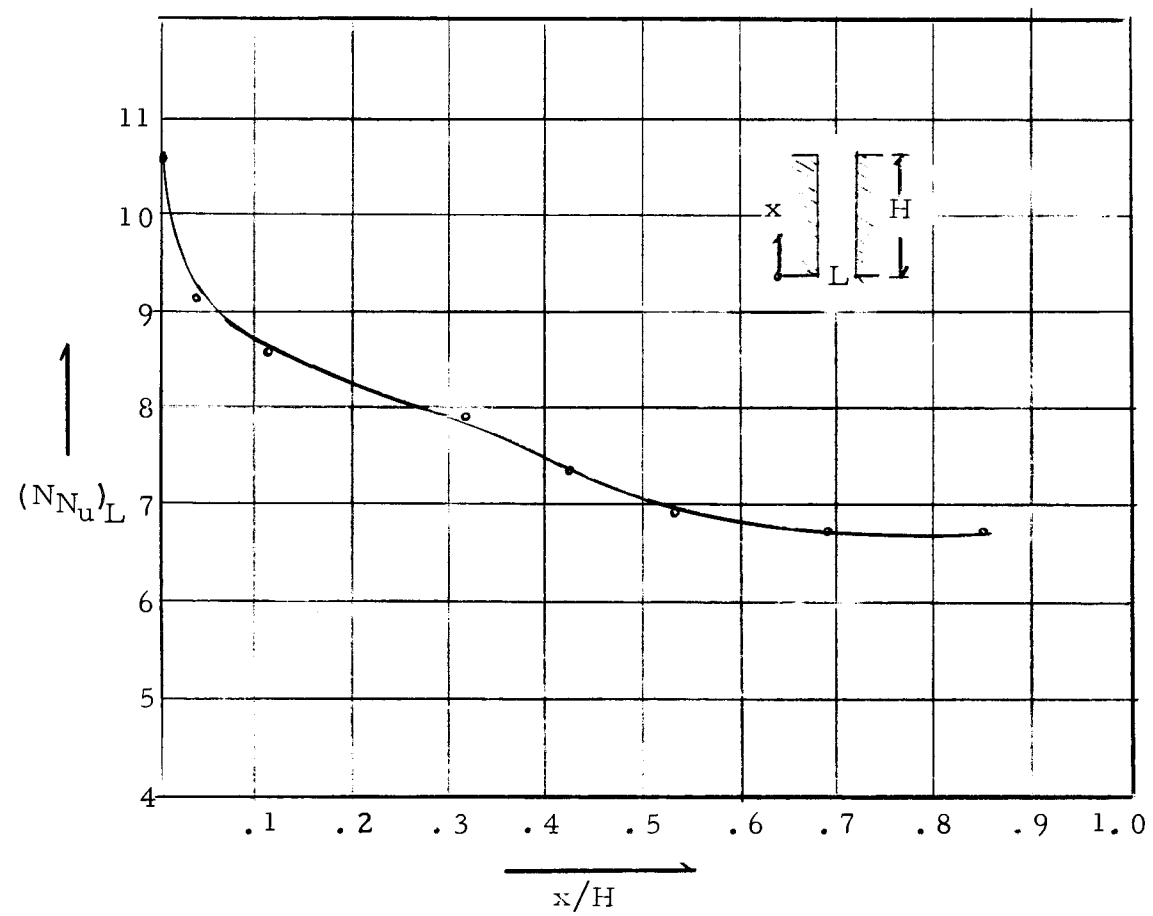


Figure 17. Local Nusselt number as a function of vertical position.

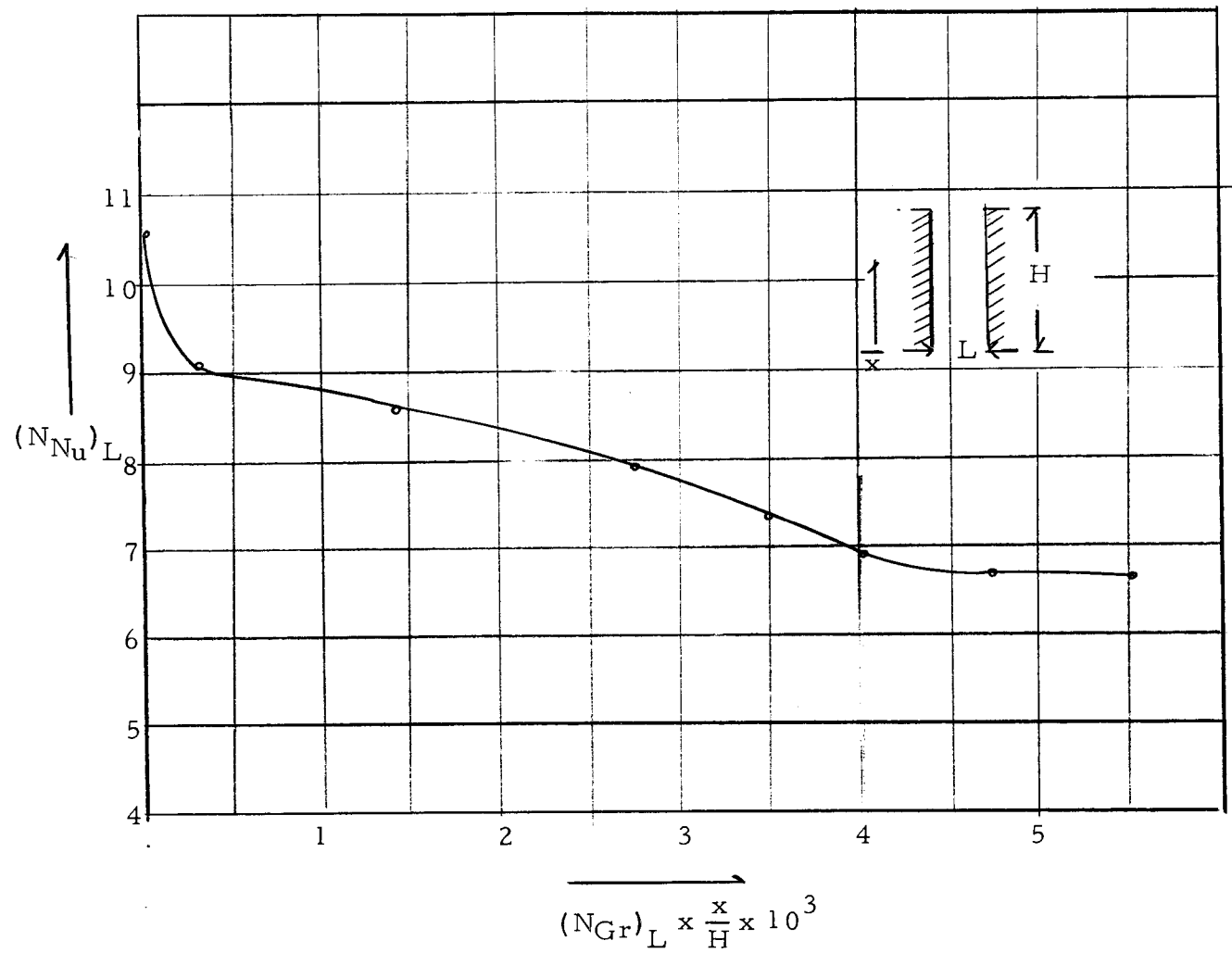


Figure 18. Local Nusselt number variation with $(N_{Gr})_L \times x/H$

$$(\bar{T}_{ave}) = \frac{1}{H} \int_0^H T_{ave} dx$$

where the local mean temperature T_{ave} is obtained from the equation (30-1). Values of T_{ave} along the vertical plates are plotted in Figure 19.

The total heat transfer rate is obtained by using the mean heat transfer coefficient \bar{h} and mean temperature \bar{T}_{ave} according to

$$Q = \bar{h}A(T_s - \bar{T}_{ave}) \quad (33)$$

The total heat loss from the surface is equal to the increase in energy of the air. The amount of energy increase of the air is calculated as follows

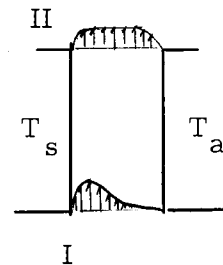
$$Q = [(\dot{m}c_p T_{ave})_{II} - (\dot{m}c_p T_{ave})_I] \cdot A \quad (34)$$

where

\dot{m} = mass rate

c_p = specific heat

T_{ave} = mean temperature



A comparison of heat transfer using equations (33) and (34) yielded values of 456 Btu/hr and 470 Btu/hr respectively; thus, the experimental error for this work was approximately three percent.

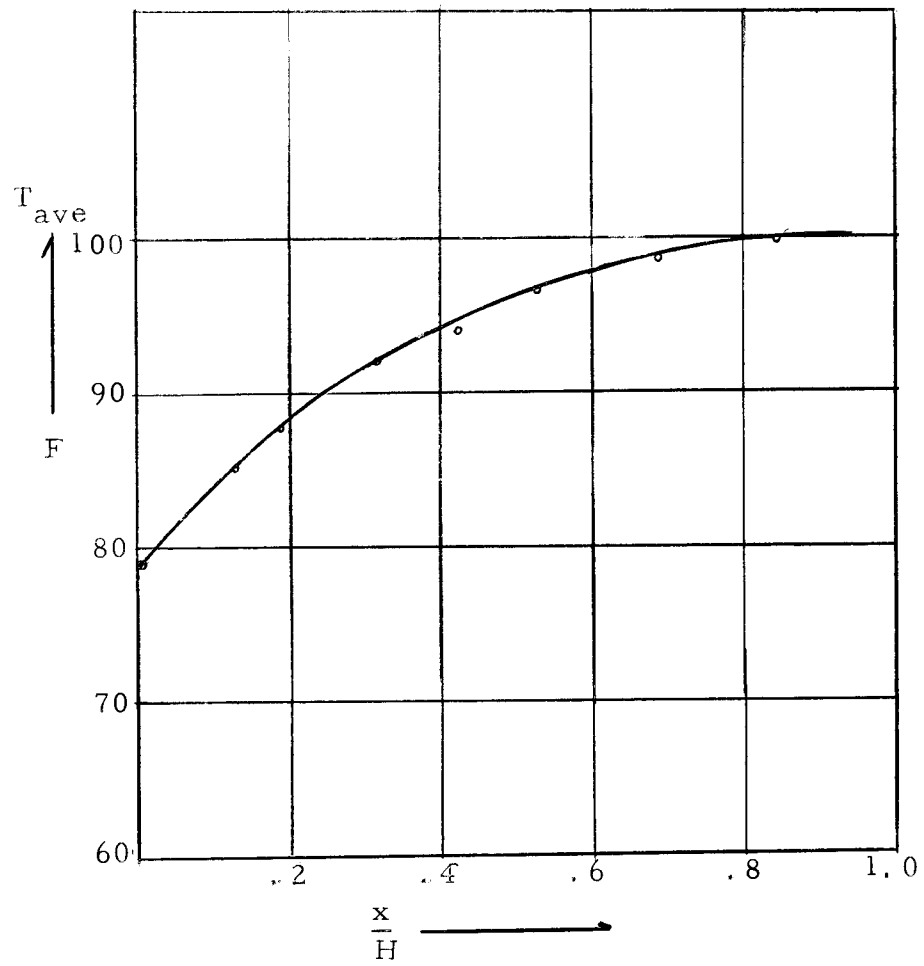


Figure 19. Local average temperature vs. vertical position.

It should be noted that all air was assumed to leave the upper portion of the apparatus and that an additional assumption was made that no heat was transferred through the plexiglass. These assumptions and possibly others are responsible for the relatively high percent error indicated above.

CONCLUSIONS

The free convection flow phenomenon in air between vertical plates, one being isothermal and the other adiabatic, has not yet been solved analytically owing to mathematical limitations.

In this experimental work, velocity and temperature variations in the air space between the vertical plates have been investigated and, with the data obtained, local convective heat transfer coefficients along the vertical plate were calculated.

It was found that different flow regimes exist, and temperature profiles are not linear. The velocity and temperature profiles in air near the hot vertical plate are similar to those obtained for a single heated plate by Schmidt and Beckmann in 1930.

It would be of interest to determine how the results obtained in this would be affected if the position and angle of these plates were varied, therefore, the author hopes that further investigations in this field will be continued to include these factors.

BIBLIOGRAPHY

1. Albers, L. U. Numerical solution of simplified boundary-value problem. In: Thirty-ninth annual report of the National Advisory Committee for Aeronautics, including technical reports. Technical report no. 1111, Appendix B. Washington, D. C., U.S. Government Printing Office, 1955. p. 73-75.
2. Dulong, P. L. and A. T. Petit. Recherches sur la mesure des temperatures, et sur les lois de la communication de la chaleur. Annales de Chimie et de Physique, 2d. ser., 7:113-154, 225-264, 337-367. 1817.
3. Griffiths, E. and A. H. Davis. The transmission of heat by radiation and convection. London, 1931. 26 p. (Great Britain. Department of Scientific and Industrial Research. Food Investigation Board. Special Report 9)
4. Lorenz, L. Über das Leitungsvermögen der Metalle fuer Wärme und Electricität. Wiedemanns Annalen der Physik und Chemi 13:582-606. 1881.
5. Nusselt, W. Die Wärmeleitfähigkeit von Wärmeisolistoffen. Mitteilungen über Forschungsarbeiten herausgegeben vom Verein deutscher Ingenieure 63 and 64:1-23. 1909.
6. Nusselt, W. and W. Juerges. Das Temperaturfeld über einer lotrecht stehenden geheizten Platte. Zeitschrift des Vereines deutscher Ingenieure 72:597-603. 1928.
7. Ostrach, S. An analysis of laminar free convection flow and heat transfer about a flat plate parallel to the direction of the generating body force. Washington, D. C., 1952. 47 p. (U.S. National Advisory Committee for Aeronautics. Technical Note 2635)
8. Ostrach, S. An analysis of laminar free convection flow and heat transfer above a flat plate parallel to the direction of the generating body force. In: Thirty-ninth annual Report of the National Advisory Committee of Aeronautics, including technical reports. Technical report no. 1111. Washington, D. C., U.S. Government Printing Office, 1955. p. 63-79.

9. Schmidt, E. and W. Beckmann. Das temperature-und Geschwindigkeitfeld vor einer wärme abgebenden senkrechten Platte bei natürlicher Konvektion. Technische Mechanik und Thermodynamik 10:341-349; 11:391-405. 1930.
10. Sparrow, E. M. and J. L. Gregg. Laminar free convection from a vertical plate with a uniform surface heat flux. Transactions of the American Society of Mechanical Engineers 78:435-550.
11. Sparrow, E. M. and J. L. Gregg. The variable fluid property problem in free convection. Transactions of the American Society of Mechanical Engineers 80:879-886. 1958..
12. Weise, R. Waermeuebergeng durch freie Konvektion an quardratischen Platte. Forschung auf dem Gebiete des Ingenieurwesens 6:281-292. 1935.

Table 1. Calibration data for quartz fiber.

Deflection, (10^{-2} mm)	Velocity (cm/sec)
2	1.83
5	2.18
7	2.80
9	2.90
10	3.00
11	3.80
13	4.24
15	4.30
16	4.52
17	4.57
20	5.30
22	5.67
25	6.26
27	6.79
29	7.00
30	7.60
32	7.79
36	8.60
40	9.50
41	9.50
43	9.70
45	10.20
48	10.90
50	11.60
54	12.80
55	13.00
58	13.20
60	13.50

Table 1. Continued.

Deflection (10^{-2} mm)	Velocity (cm/sec)
65	14.00
66	14.00
68	14.20
70	14.30
72	14.50
75	15.00
79	15.40
80	15.50
83	16.09
85	16.31
88	17.00
90	17.90
93	18.00
95	18.10
96	18.20
100	18.60
102	19.00
105	19.21
108	19.72
110	20.10
115	20.70
117	21.10
120	21.50
124	22.00
127	22.51
130	23.30
132	23.31
135	23.80

Table 1. Continued.

Deflection, (10^{-2} mm)	Velocity (cm/sec)
139	24.20
141	24.50
143	25.00
148	24.90
150	25.70
153	26.11
155	26.42
157	26.50
160	26.70
163	27.22
165	27.30
168	27.60
170	27.90
172	28.00
175	28.60
176	28.60
178	28.70
181	29.80
185	30.00
186	30.00
188	30.50
190	30.60
193	31.00
195	31.20
198	31.42
200	31.80
203	32.21
205	32.91

Table 1. Continued.

Deflection, (10^{-2} mm)	Velocity (cm/sec)
208	32.80
210	33.20
220	34.21
225	34.70
229	35.10
232	35.40
240	36.42
250	37.82
255	38.42
268	38.81
270	39.10
275	39.50
280	39.90
295	41.10
298	41.10
305	41.72
315	42.15
340	43.60
360	44.12

Table 2. Experimental velocity data.

y (mm)	y/L	(10^{-2} mm)	V (cm/sec)	V/V _{ave}
.635	.04			
1.270	.08	30	7.6	0.62
1.905	.12	60	13.5	1.10
2.540	.16	75	15.0	1.23
3.175	.20	85	16.3	1.34
3.810	.24	95	18.1	1.48
4.445	.28	100	18.6	1.52
5.080	.32	103	19.0	1.55
5.715	.36	100	18.6	1.52
6.350	.40	97	18.3	1.50
6.985	.44	93	17.6	1.48
7.620	.48	88	17.0	1.39
8.255	.52	87	16.9	1.38
8.890	.56	83	16.0	1.31
9.525	.60	80	15.5	1.27
10.160	.64	79	15.4	1.26
10.795	.68	75	15.0	1.23
11.430	.72	70	14.3	1.18
12.065	.76	50	11.2	0.91
12.700	.80	30	7.6	0.62
13.336	.84	20	5.3	0.43
13.970	.88	10	3.0	0.24
14.605	.92	0	0	0
15.240	.96	0	0	0
15.895	1.00	0	0	0

* $x = 0.25$ in. $V_{ave} = 12.2$ cm/sec.

Table 2. Continued.*

y (mm)	y/L	(10^{-2} mm)	V (cm/sec)	V/V _{ave}
.635	.04			
1.270	.08	47	10.2	0.70
1.905	.12	65	14.0	0.95
2.540	.16	100	18.6	1.26
3.175	.20	115	20.7	1.41
3.810	.24	125	22.3	1.51
4.44	.28	133	23.3	1.59
5.080	.32	128	22.6	1.54
5.715	.36	127	22.5	1.53
6.350	.40	121	21.5	1.47
6.985	.44	114	20.7	1.41
7.620	.48	113	20.4	1.39
8.255	.52	110	20.1	1.37
8.890	.56	108	19.7	1.34
9.525	.60	103	19.0	1.29
10.160	.64	100	18.6	1.26
10.750	.68	90	17.9	1.21
11.430	.72	80	15.5	1.05
12.065	.76	58	13.2	0.90
12.70	.80	45	10.2	0.69
13.336	.84	25	6.0	0.41
13.970	.88	12	3.0	0.20
14.605	.92	6	1.6	0.10
15.240	.96	0	0	0
15.895	1.00	0	0	0

* $x = 0.50$ in. $V_{ave} = 14.7$ cm/sec

Table 2. Continued.*

y(mm)	y/L	(10 ⁻² mm)	V (cm/sec)	V/V _{ave}
.635	.04			
1.270	.08	50	11.6	0.73
1.905	.12	70	14.3	0.89
2.540	.16	105	19.2	1.21
3.175	.20	125	22.3	1.41
3.810	.24	135	23.8	1.49
4.445	.28	140	24.2	1.52
5.080	.32	139	24.1	1.51
5.715	.36	137	23.9	1.50
6.350	.40	135	23.8	1.495
6.985	.44	132	23.4	1.47
7.620	.48	130	23.0	1.44
8.255	.52	125	22.3	1.40
8.890	.56	121	21.7	1.36
9.525	.60	115	20.8	1.31
10.160	.64	107	19.5	1.23
10.795	.68	96	18.2	1.14
10.430	.72	85	16.3	1.03
12.065	.76	60	13.5	0.85
12.700	.80	50	11.2	0.70
13.336	.84	40	9.5	0.60
13.970	.88	20	5.3	0.33
14.605	.92	10	3.0	0.18
15.240	.96	6	1.5	0.09
15.895	1.00	0	0	0

* $x = 1 \text{ in.}$ $V_{\text{ave}} = 15.9$

Table 2. Continued.*

y (mm)	y/L	(10 ⁻² mm)	V (cm/sec)	V/V _{ave}
.695	.04			
1.270	.08	60	13.5	.726
1.905	.12	85	16.3	.937
2.540	.16	110	20.0	1.15
3.175	.20	130	23.0	1.32
3.810	.24	145	24.7	1.42
4.445	.28	155	26.3	1.51
5.080	.32	165	27.3	1.57
5.715	.36	170	27.9	1.60
6.350	.40	165	27.3	1.57
6.985	.44	155	26.3	1.51
7.620	.48	142	24.4	1.40
8.255	.52	128	22.7	1.30
8.890	.56	125	22.0	1.26
9.525	.60	120	21.5	1.24
10.160	.64	110	20.0	1.15
10.795	.68	100	18.6	1.07
11.430	.72	88	17.6	1.01
12.065	.76	65	14.0	.88
12.700	.80	55	13.0	.747
13.336	.84	45	10.2	.584
13.970	.88	25	6.6	.375
14.605	.92	14	4.0	.23
15.240	.96	9	2.3	.132
15.895	1.00	0	0	0

*
x = 5 in. V_{ave} = 17.4

Table 2. Continued. *

y (mm)	y/L	(10 ⁻² mm)	V (cm/sec)	V/V _{ave}
.635	.04			
1.270	.08	65	14.0	0.74
1.905	.12	90	17.9	0.90
2.540	.16	115	20.8	1.1
3.175	.20	140	24.2	1.29
3.810	.24	160	26.75	1.42
4.445	.28	180	29.3	1.57
5.080	.32	182	29.8	1.59
5.715	.36	185	30.0	1.60
6.350	.40	178	29.1	1.55
6.985	.44	170	27.9	1.49
7.620	.48	160	26.75	1.43
8.255	.52	150	25.7	1.38
8.890	.56	140	24.2	1.30
9.525	.60	130	23.0	1.23
10.160	.64	115	20.8	1.11
10.795	.68	105	19.2	1.03
11.430	.72	90	17.9	0.90
12.065	.76	70	14.3	0.76
12.700	.80	55	13.0	0.69
13.336	.84	48	10.9	0.58
13.970	.88	30	7.6	0.40
14.605	.92	19	5.3	0.28
15.240	.96	10	3.0	0.16
15.895	1.00	0	0	0

* X = 7 in. V_{ave} = 18.7

Table 2. Continued. *

y (mm)	y/L	(10 ⁻² mm)	V (cm/sec)	V/V _{ave}
.635	.04			
1.270	.08	80	15.5	0.715
1.905	.12	100	18.6	0.85
2.540	.16	125	22.0	1.01
3.175	.20	150	25.7	1.18
3.810	.24	170	27.9	1.28
4.445	.28	183	29.8	1.37
5.080	.32	190	30.6	1.41
5.715	.36	200	31.8	1.47
6.350	.40	210	33.2	1.52
6.985	.44	208	32.8	1.51
7.620	.48	203	32.2	1.48
8.255	.52	197	31.4	1.44
8.890	.56	186	30.0	1.38
9.525	.60	170	27.9	1.29
10.160	.64	160	26.7	1.22
10.795	.68	139	24.2	1.12
11.430	.72	120	21.5	0.99
12.065	.76	108	19.8	0.91
12.700	.80	93	18.0	0.83
13.336	.84	79	15.4	0.71
13.970	.88	54	12.8	0.59
14.650	.92	36	8.6	0.4
15.240	.96	15	4.3	0.19
15.895	1.00	0	0	0

* $x = 12$ in. $V_{ave} = 21.7$ cm/sec

Table 2. Continued.*

y (mm)	y/L	(10^{-2} mm)	V (cm/sec)	V/V _{ave}
.635	.04			
1.270	.08	98	18.2	0.70
1.905	.12	124	22.3	0.86
2.540	.16	155	26.4	1.02
3.175	.20	185	30.0	1.16
3.810	.24	210	33.2	1.29
4.445	.28	225	34.8	1.35
5.080	.32	230	35.5	1.38
5.715	.36	235	36.3	1.41
6.350	.40	238	36.8	1.43
6.985	.44	240	36.9	1.44
7.620	.48	233	35.8	1.39
8.255	.52	227	35.0	1.36
8.890	.56	220	34.3	1.33
9.525	.60	208	32.0	1.28
10.160	.64	190	30.6	1.19
10.795	.68	175	28.6	1.11
11.430	.72	150	25.8	1.00
12.065	.76	140	24.2	0.94
12.700	.80	130	22.7	0.88
13.336	.84	110	20.1	0.78
13.970	.88	90	17.9	0.69
14.650	.92	65	14.0	0.55
15.240	.96	20	5.4	0.21
15.895	1.00	0	0	0

* $x = 16$ in. $V_{ave} = 25.74$ cm/sec.

Table 2. Continued.*

y (mm)	y/L	(10^{-2} mm)	V (cm/sec)	V/V _{ave}
.635	.04			
1.270	.08	105	19.2	.68
1.905	.12	130	23.0	.82
2.540	.16	165	27.3	.97
3.175	.20	195	31.3	1.12
3.810	.24	215	33.8	1.21
4.445	.28	230	35.5	1.26
5.080	.32	236	36.4	1.30
5.715	.36	245	37.3	1.33
6.350	.40	252	38.0	1.35
6.985	.44	258	38.7	1.38
7.620	.48	255	38.3	1.36
8.255	.52	250	37.8	1.35
8.890	.56	248	37.6	1.34
9.525	.60	245	37.3	1.33
10.160	.64	230	35.5	1.27
10.795	.68	220	34.3	1.22
11.430	.72	205	32.5	1.16
12.065	.76	182	29.7	1.06
12.70	.80	160	26.7	.96
13.336	.84	146	25.2	.90
13.970	.88	105	19.2	.68
14.605	.92	75	15.0	.53
15.240	.96	30	7.6	.27
15.895	1.00	0	0	0

* $x = 20$ in. $V_{ave} = 28.0$ cm/sec

Table 2. Continued.*

y (mm)	y/L	(10 ⁻² mm)	V (cm/sec)	V/V _{ave}
.635	.04			
1.270	.08	110	20.0	.68
1.905	.12	150	25.8	.875
2.540	.16	180	29.3	.995
3.175	.20	215	33.8	1.140
3.810	.24	240	36.9	1.250
4.445	.28	250	37.8	1.280
5.080	.32	265	39.1	1.320
5.715	.36	280	40.2	1.360
6.350	.40	290	40.8	1.380
6.985	.44	295	41.2	1.390
7.620	.48	290	40.8	1.380
8.255	.52	285	40.5	1.370
8.890	.56	275	39.7	1.340
9.525	.60	260	38.7	1.310
10.160	.64	245	37.3	1.270
10.795	.68	230	35.5	1.210
11.430	.72	205	32.5	1.110
12.065	.76	190	30.6	1.040
12.700	.80	170	27.9	.95
13.336	.84	150	25.8	.87
13.970	.88	105	19.2	.66
14.650	.92	78	15.3	.52
15.240	.96	20	5.4	.18
15.895	1.00	0	0	0

* $x = 26$ in. $V_{ave} = 29.6$

Table 2. Continued.*

y (mm)	y/L	(10 ⁻² mm)	V (cm/sec)	V/V _{ave}
.635	.04			
1.270	.08	120	21.5	.67
1.905	.12	170	27.9	.86
2.540	.16	210	33.2	1.03
3.175	.20	240	36.9	1.14
3.810	.24	285	40.5	1.35
4.445	.28	315	42.2	1.31
5.080	.32	345	43.0	1.33
5.715	.36	350	43.2	1.34
6.350	.40	355	43.3	1.34
6.985	.44	360	43.4	1.35
7.620	.48	355	43.3	1.34
8.255	.52	345	43.0	1.33
8.890	.56	330	42.9	1.33
9.525	.60	315	42.2	1.31
10.160	.64	295	41.2	1.28
10.795	.68	275	39.7	1.23
11.430	.72	245	37.3	1.16
12.065	.76	215	33.8	1.05
12.70	.80	185	30.0	0.93
13.336	.84	160	26.7	0.83
13.970	.88	120	21.5	0.67
14.650	.92	85	16.5	0.51
15.240	.96	25	6.7	0.21
15.895	1.00	0	0	0

* $x = 32$ in. $V_{ave} = 32.2$ cm/sec.

Table 3. Temperature data.*

y (mm)	y/L	T _f	θ
0	0	.	0
1.000	.063	95.3	.667
1.635	.103	88.7	.801
2.910	.183	83.7	.905
4.18	.263	80.3	.973
5.45	.343	76.3	1.050
6.74	.423	74.3	1.090
8.00	.503	74.0	1.110
9.26	.583	74.0	1.110
10.52	.663	74.0	1.110
11.79	.743	74.0	1.110
13.05	.823	74.0	1.110
14.31	.903	74.0	1.110
15.57	.983	74.0	1.110
15.895	1.000	74.0	1.110

* L = 15.895 mm

T_s = 128 FT_{ave} = 79 F

x = .25 in.

T_{amb} = 74 F

Table 3. Continued. *

y (mm)	y/L	T_f	θ
0	0		0
1.000	.063	100.3	.575
1.635	.103	94.7	.692
2.910	.183	87.3	.845
4.18	.183	82.0	.955
5.45	.263	76.7	1.065
6.74	.343	75.3	1.095
8.00	.423	74.3	1.115
9.26	.583	74.0	1.120
10.52	.663	74.0	1.120
11.79	.743	74.0	1.120
13.05	.823	74.0	1.120
14.31	.903	74.0	1.120
15.57	.983	74.0	1.120
15.895	1.000	74.0	1.120

* $L = 15.895$ mm $T_s = 128$ F $T_{ave} = 79.8$ F $x = .5$ in. $T_{amb} = 74$ F

Table 3. Continued. *

y (mm)	y/L	T_f	θ
0	0		0
1.000	.063	100.3	.596
1.635	.103	98.3	.642
2.910	.183	88.7	.846
4.180	.263	82.7	.976
5.450	.343	78.3	1.070
6.740	.423	76.3	1.110
8.000	.503	75.3	1.130
9.260	.583	75.0	1.140
10.520	.663	75.0	1.140
11.790	.743	75.0	1.140
13.050	.823	75.0	1.140
14.310	.903	74.7	1.145
15.570	.983	74.7	1.145
15.895	1.000	74.7	1.145

* $L = 15.895$ mm $T_s = 128$ F $T_{ave} = 81.5$ F $x = 1$ in $T_{amb} = 74$ F

Table 3. Continued.*

y (mm)	y/L	T_f	θ
0	0		0
1.000	.063	104.7	.542
1.635	.103	101.3	.622
2.910	.183	95.0	.766
4.180	.263	90.0	.884
5.450	.343	85.0	1.000
6.740	.423	81.7	1.078
8.000	.503	80.0	1.113
9.260	.583	78.3	1.160
10.520	.663	77.7	1.170
11.790	.743	77.0	1.185
13.050	.823	76.7	1.191
14.310	.903	76.3	1.200
15.570	.983	76.3	1.200
15.895	1.000	76.3	1.200

* $L = 15.895$ mm $T_s = 128$ F $T_{ave} = 85$ F $x = 5$ in $T_{amb} = 74$ F

Table 3. Continued.*

y (mm)	y/L	T_f	θ
0	0		0
1.000	.063	106.7	.527
1.635	.103	103.7	.602
2.910	.183	99.7	.700
4.180	.263	94.7	.826
5.450	.343	90.3	.933
6.740	.423	85.7	1.050
8.000	.503	83.0	1.110
9.260	.583	81.3	1.150
10.520	.663	79.7	1.190
11.790	.743	78.7	1.220
13.050	.823	77.7	1.245
14.310	.903	77.3	1.250
15.570	.983	77.3	1.250
15.895	1.000	77.3	1.250

* $L = 15.895$ mm $T_s = 128$ F $T_{ave} = 87.6$ F $x = 7$ in $T_{amb} = 74$ F

Table 3. Continued.*

y (mm)	y/L	T_f	θ
0	0		0
1.000	.063	109.7	.500
1.635	.103	106.5	.587
2.910	.183	102.2	.710
4.180	.263	97.8	.835
5.450	.343	94.0	.942
6.740	.423	91.3	1.020
8.000	.503	89.0	1.080
9.260	.583	86.5	1.150
10.520	.663	84.7	1.205
11.790	.743	83.3	1.240
13.050	.823	82.3	1.275
14.310	.903	81.3	1.301
15.570	.983	81.0	1.310
15.895	1.000	81.0	1.310

* $L = 15.895$ mm $T_s = 127.3$ F $T_{ave} = 92$ F $x = 12$ in. $T_{amb} = 74$ F

Table 3. Continued.*

y (mm)	y/L	T_f	θ
0	0		0
1.000	.063	112.0	.460
1.635	.103	109.7	.528
2.910	.183	105.5	.655
4.180	.263	103.0	.730
5.450	.343	99.7	.829
6.740	.423	95.0	.965
8.000	.503	92.3	1.050
9.260	.583	89.7	1.130
10.520	.663	87.4	1.200
11.790	.743	85.5	1.255
13.050	.823	84.7	1.280
14.310	.903	83.5	1.310
15.570	.983	82.5	1.340
15.895	1.000	82.5	1.340

* $L = 15.895$ mm $T_s = 127.3$ $T_{ave} = 94$ F $x = 16$ in. $T_{amb} = 74$ F

Table 3. Continued.*

y (mm)	y/L	T_f	θ
0	0	0	0
1.000	.063	113.7	.432
1.635	.103	110.3	.543
2.910	.183	108.0	.619
4.180	.263	104.7	.725
5.450	.343	101.3	.845
6.740	.423	98.0	.944
8.000	.503	94.7	1.050
9.260	.583	92.0	1.140
10.520	.663	89.7	1.210
11.790	.743	88.0	1.270
13.050	.823	86.0	1.330
14.310	.903	84.3	1.390
15.570	.983	83.7	1.410
15.895	1.000	83.7	1.410

* $L = 15.895$ mm $T_s = 127$ F $T_{ave} = 96.3$ F $x = 20$ in. $T_{amb} = 74$ F

Table 3. Continued.*

y (mm)	y/L	T_f	θ
0	0		0
1.000	.063	114.7	.420
1.635	.103	112.3	.507
2.910	.183	108.3	.650
4.180	.263	105.0	.770
5.450	.343	102.3	.867
6.740	.423	99.7	.962
8.000	.503	96.5	1.070
9.260	.583	94.0	1.160
10.520	.663	91.7	1.250
11.790	.743	89.3	1.330
13.050	.823	87.7	1.390
14.310	.903	86.0	1.450
15.570	.983	84.7	1.500
15.895	1.000	84.7	1.500

* $L = 15.895$ mm $T_s = 126.4$ F $T_{ave} = 98.6$ F $x = 26$ in. $T_{amb} = 74$ F

Table 3. Continued.*

y (mm)	y/L	T_f	θ
0	0		0
1.000	.063	115.3	.420
1.635	.103	112.7	.534
2.910	.183	110.0	.583
4.180	.263	107.0	.730
5.450	.343	104.3	.837
6.740	.423	101.7	.935
8.000	.503	98.7	1.050
9.260	.583	96.0	1.180
10.520	.663	93.7	1.240
11.790	.743	92.0	1.300
13.050	.823	90.7	1.350
14.310	.903	89.7	1.390
15.570	.983	89.3	1.410
15.895	1.000	89.3	1.410

* $L = 15.895$ mm $T_s = 126.4$ F $T_{ave} = 100$ F $x = 32$ in. $T_{amb} = 74$ F

Table 4. Local Nusselt numbers at various vertical positions.

x (inch)	Nusselt number
. 25	10. 6
1. 00	9. 12
5. 00	8. 60
12. 00	7. 94
16. 00	7. 35
20. 00	6. 88
26. 00	6. 70
32. 00	6. 67

Table 5. Local Grashof numbers at various vertical positions.

x (inch)	$(N_{Gr})_L \times \frac{x}{H}$	$(N_{Nu})_L$
. 25	80	10. 6
1. 00	320	9. 12
5. 00	1410	8. 60
12. 00	2760	7. 94
16. 00	3480	7. 35
20. 00	4000	6. 88
26. 00	4740	6. 70
32. 00	5500	6. 67